2007 SEG Meeting

Numerical Simulation of 3D DC and AC Resistivity Logging Measurements in Deviated Wells using an hp-Adaptive Goal-Oriented Finite Element Formulation.

D. Pardo, M. J. Nam, C. Torres-Verdín, M. Paszynski, V. M. Calo

hp-FE TEAM: D. Pardo, M. Paszynski, M. J. Nam, Ch. Michler,
R. Abdollah-Pour, L. Demkowicz, C. Torres-Verdín

September 26, 2007

Department of Petroleum and Geosystems Engineering

THE UNIVERSITY OF TEXAS AT AUSTIN

OVERVIEW

1. **Motivation: Simulation of resistivity logging measurements in deviated wells.**
2. **Methodology:**
   - **Fourier series expansion.**
   - **Non-orthogonal system of coordinates.**
   - **2D goal-oriented self-adaptive hp-FEM.**
   - **Verification of the methodology.**
3. **Numerical results:**
   - **3D DC through-casing measurements in deviated wells.**
   - **3D DC dual laterolog measurements in deviated wells.**
   - **3D AC wireline and LWD measurements in deviated wells.**
4. **Conclusions and future work.**

MOTIVATION (APPLICATIONS)

Deviated Wells (Forward Problem)

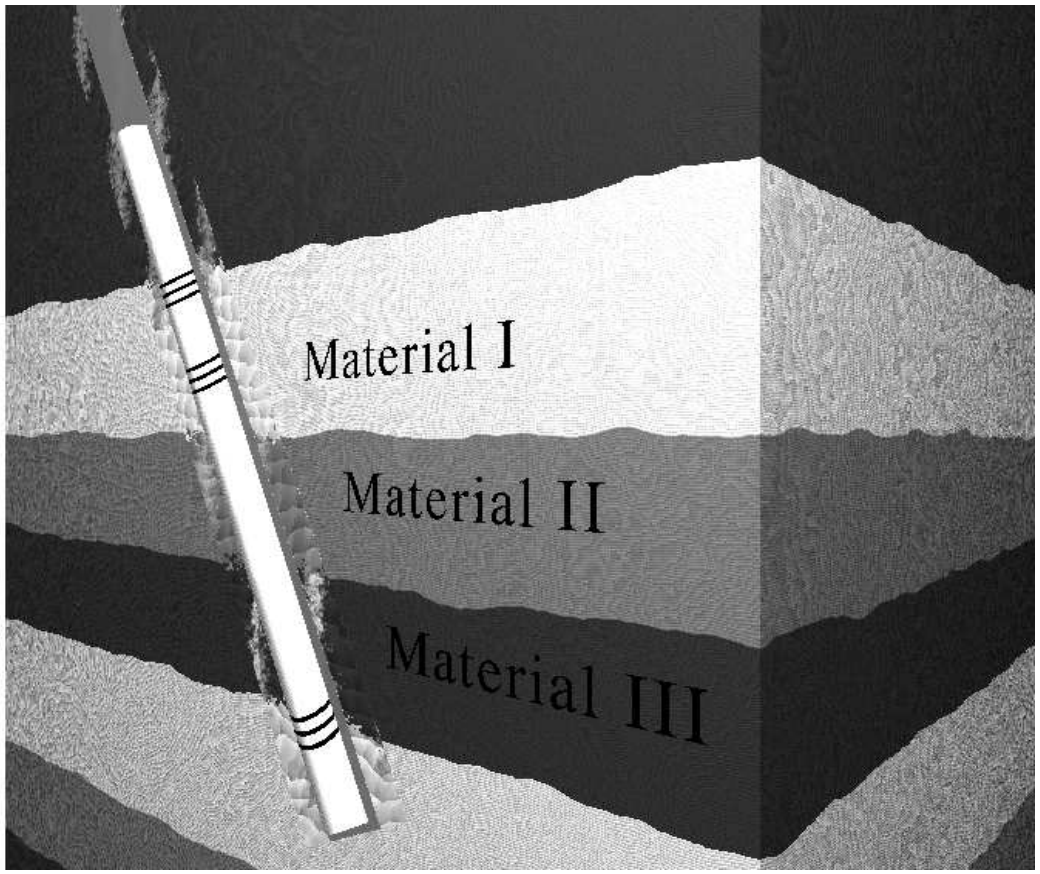

- Dip Angle
- Invasion
- Anisotropy
- Triaxial Induction
- Eccentricity
- Laterolog
- Through-Casing
- Induction-LWD
- Induction-Wireline
- Inverse Problems
- Multi-Physics

Objective: Find solution at the receiver antennas.

METHODOLOGY: MAIN IDEA

Non-Orthogonal System of Coordinates

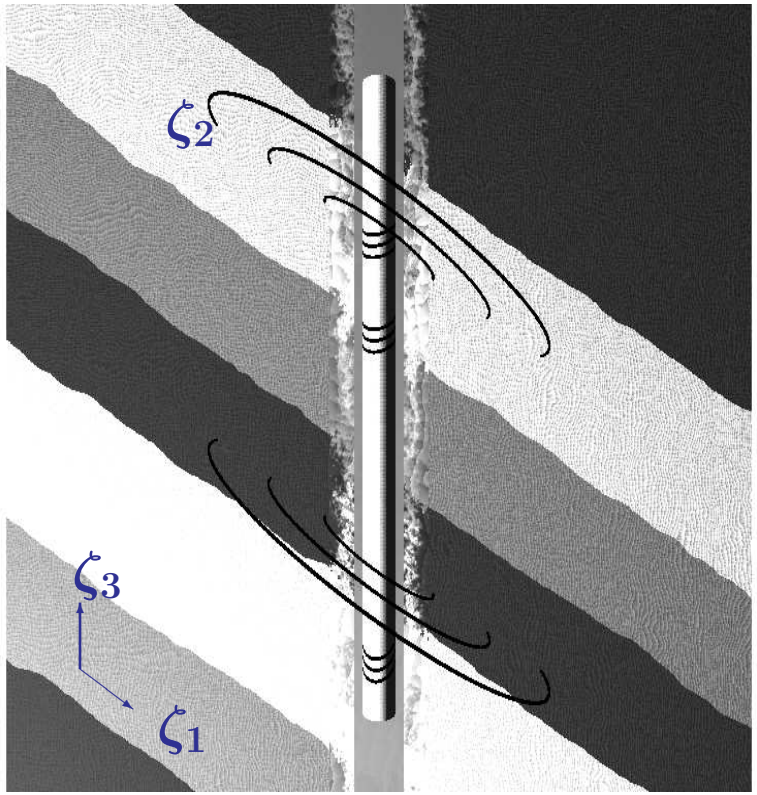

Material coefficients are constant with respect to the quasi-azimuthal direction ζ_2

Fourier Series Expansion in ζ_2

DC Problems: $-\nabla\sigma\nabla u = f$

$$u(\zeta_1,\zeta_2,\zeta_3) = \sum_{l=-\infty}^{l=\infty} u_l(\zeta_1,\zeta_3)e^{jl\zeta_2}$$

$$\sigma(\zeta_1,\zeta_2,\zeta_3) = \sum_{m=-\infty}^{m=\infty} \sigma_m(\zeta_1,\zeta_3)e^{jm\zeta_2}$$

$$f(\zeta_1,\zeta_2,\zeta_3) = \sum_{n=-\infty}^{n=\infty} f_n(\zeta_1,\zeta_3)e^{jn\zeta_2}$$

Fourier modes $e^{jl\zeta_2}$ are orthogonal high-order basis functions that are (almost) invariant with respect to the gradient operator.

METHODOLOGY: NEW SYSTEM OF COORDINATES

Cartesian system of coordinates: $\mathrm{x} = (x_1, x_2, x_3)$.

New non-orthogonal system of coordinates: $\zeta = (\zeta_1, \zeta_2, \zeta_3)$.

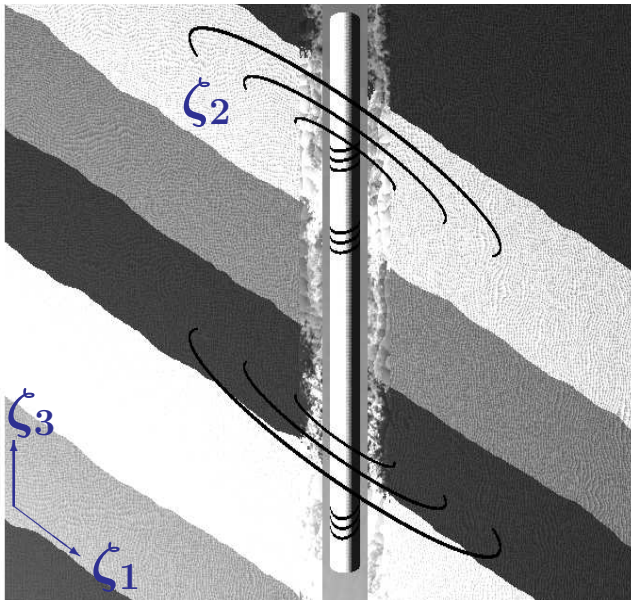

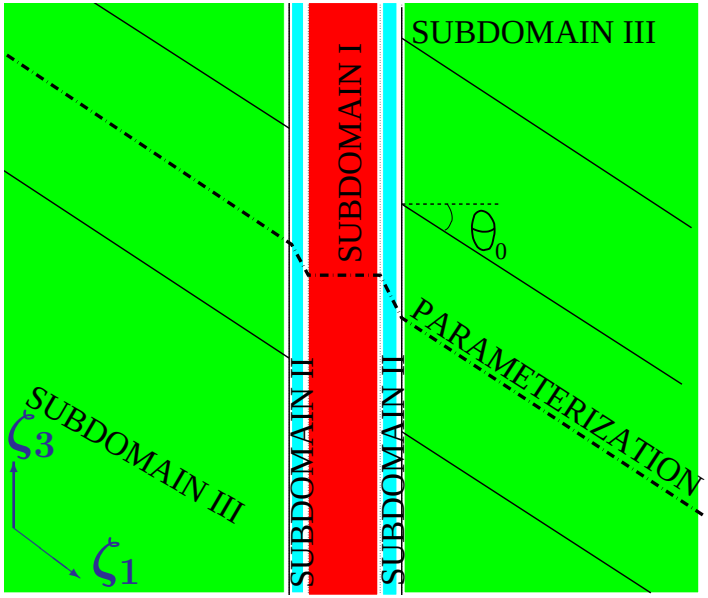

Subdomain I ; **Subdomain II** ; **Subdomain III**

$$\begin{cases} x_1 = \zeta_1 \cos\zeta_2 \\ x_2 = \zeta_1 \sin\zeta_2 \\ x_3 = \zeta_3 \end{cases} ; \quad \begin{cases} x_1 = \zeta_1 \cos\zeta_2 \\ x_2 = \zeta_1 \sin\zeta_2 \\ x_3 = \zeta_3 + \tan\theta_0 \dfrac{\zeta_1 - \rho_1}{\rho_2 - \rho_1}\rho_2 \end{cases} ; \quad \begin{cases} x_1 = \zeta_1 \cos\zeta_2 \\ x_2 = \zeta_1 \sin\zeta_2 \\ x_3 = \zeta_3 + \tan\theta_0\zeta_1 \end{cases}$$

METHODOLOGY: NEW SYSTEM OF COORDINATES

Final Variational Formulation

We define the Jacobian matrix $\mathcal{J} = \dfrac{\partial(x_1, x_2, x_3)}{\partial(\zeta_1, \zeta_2, \zeta_3)}$ and its determinant $|\mathcal{J}| = \det(\mathcal{J})$.

Variational formulation in the new system of coordinates:

$$\begin{cases} \text{Find } u \in u_D + H^1_D(\Omega) \text{ such that:} \\ \left\langle \dfrac{\partial v}{\partial \zeta} \, , \, \tilde{\sigma} \dfrac{\partial u}{\partial \zeta} \right\rangle_{L^2(\Omega)} = \left\langle v \, , \, \tilde{f} \right\rangle_{L^2(\Omega)} \quad \forall v \in H^1_D(\Omega) \, , \end{cases}$$

where:

$$\tilde{\sigma} := \mathcal{J}^{-1} \sigma \mathcal{J}^{-1^T} |\mathcal{J}| \quad ; \quad \tilde{f} := f |\mathcal{J}| \, .$$

Same variational formulation with new materials and load data

METHODOLOGY: FOURIER SERIES EXPANSION

For a mono-modal test function $v = v_k e^{jk\zeta_2}$, we have:

$$\begin{cases} \textbf{Find } u \in u_D + H^1_D(\Omega) \textbf{ such that:} \\ \displaystyle\sum_{m,n} \left\langle \left(\frac{\partial v}{\partial \zeta}\right)_k e^{jk\zeta_2} \,,\, \tilde{\sigma}_m \left(\frac{\partial u}{\partial \zeta}\right)_n e^{j(m+n)\zeta_2} \right\rangle_{L^2(\Omega)} = \\ \displaystyle = \sum_l \left\langle v_k e^{jk\zeta_2} \,,\, \tilde{f}_l e^{jl\zeta_2} \right\rangle_{L^2(\Omega)} \quad \forall v_k e^{jk\zeta_2} \in H^1_D(\Omega) \end{cases}$$

Using the L^2-orthogonality of Fourier modes:

$$\begin{cases} \textbf{Find } u \in u_D + H^1_D(\Omega) \textbf{ such that:} \\ \displaystyle\sum_n \left\langle \left(\frac{\partial v}{\partial \zeta}\right)_k \,,\, \tilde{\sigma}_{k-n} \left(\frac{\partial u}{\partial \zeta}\right)_n \right\rangle_{L^2(\Omega_{2D})} = \left\langle v_k \,,\, \tilde{f}_k \right\rangle_{L^2(\Omega_{2D})} \quad \forall v_k \end{cases}$$

METHODOLOGY: FOURIER SERIES EXPANSION

Five Fourier modes are enough to represent EXACTLY the new material coefficients.

$$\tilde{\boldsymbol{\sigma}}(\zeta_1,\zeta_2,\zeta_3) = \sum_{m=-2}^{m=2} \tilde{\boldsymbol{\sigma}}_m(\zeta_1,\zeta_3) e^{jm\zeta_2}$$

METHODOLOGY: FOURIER SERIES EXPANSION

Five Fourier modes are enough to represent EXACTLY the new material coefficients.

$$\tilde{\sigma}(\zeta_1,\zeta_2,\zeta_3) = \sum_{m=-2}^{m=2} \tilde{\sigma}_m(\zeta_1,\zeta_3) e^{jm\zeta_2}$$

Final Variational Formulation

$$\begin{cases} \text{Find } u \in u_D + H^1_D(\Omega) \text{ such that:} \\ \displaystyle\sum_{n=k-2}^{n=k+2} \left\langle \left(\frac{\partial v}{\partial \zeta}\right)_k , \tilde{\sigma}_{k-n} \left(\frac{\partial u}{\partial \zeta}\right)_n \right\rangle_{L^2(\Omega_{2D})} = \left\langle v_k , \tilde{f}_k \right\rangle_{L^2(\Omega_{2D})} \quad \forall v_k \end{cases}$$

METHODOLOGY: VARIATIONAL FORMULATION

Five Fourier modes are enough to represent EXACTLY the new material coefficients.

Direct Current:

Find $u \in u_D + H^1_D(\Omega)$ such that:

$$\sum_{n=k-2}^{n=k+2} \left\langle \left(\frac{\partial v}{\partial \zeta}\right)_k , \tilde{\sigma}_{k-n} \left(\frac{\partial u}{\partial \zeta}\right)_n \right\rangle_{L^2(\Omega_{2D})} = \left\langle v_k , \tilde{f}_k \right\rangle_{L^2(\Omega_{2D})} \qquad \forall v_k$$

Alternate Current:

Find $(\mathrm{E})_s \in H_{\Gamma_E}(\mathrm{curl};\Omega)$ such that:

$$\sum_{n=s-2}^{n=s+2} \left\langle (\nabla^\zeta \times \mathrm{F})_s , (\tilde{\mu}^{-1})_{s-n} (\nabla^\zeta \times \mathrm{E})_l \right\rangle_{L^2(\Omega_{2D})} - \left\langle \mathrm{F}_s , (\tilde{k^2})_{s-n} \mathrm{E}_l \right\rangle_{L^2(\Omega_{2D})} = -j\omega \left\langle \mathrm{F}_s , (\tilde{\mathrm{J}}^{imp})_s \right\rangle_{L^2(\Omega_{2D})} \qquad \forall \mathrm{F}_s$$

METHODOLOGY: IMPLEMENTATION

Example (7 Fourier Modes)

$$\sum_{n=k-2}^{n=k+2} \underbrace{\left\langle \left(\frac{\partial v}{\partial \zeta}\right)_k \, , \, \tilde{\sigma}_{k-n} \left(\frac{\partial u}{\partial \zeta}\right)_n \right\rangle_{L^2(\Omega_{2D})}}_{(k,k-n,n)} = \left\langle v_k \, , \, \tilde{f}_k \right\rangle_{L^2(\Omega_{2D})}$$

Stiffness Matrix:

$$\begin{pmatrix}
(-3,0,-3) & (-3,-1,-2) & (-3,-2,-1) & 0 & 0 & 0 & 0 \\
(-2,1,-3) & (-2,0,-2) & (-2,-1,-1) & (-2,-2,0) & 0 & 0 & 0 \\
(-1,2,-3) & (-1,1,-2) & (-1,0,-1) & (-1,-1,0) & (-1,-2,1) & 0 & 0 \\
0 & (0,2,-2) & (0,1,-1) & (0,0,0) & (0,-1,1) & (0,-2,2) & 0 \\
0 & 0 & (1,2,-1) & (1,1,0) & (1,0,1) & (1,-1,2) & (1,-2,3) \\
0 & 0 & 0 & (2,2,0) & (2,1,1) & (2,0,2) & (2,-1,3) \\
0 & 0 & 0 & 0 & (3,2,1) & (3,1,2) & (3,0,3)
\end{pmatrix}$$

METHODOLOGY: 2D hp-FEM

A Self-Adaptive Goal-Oriented hp-FEM

Optimal 2D Grid
(Through Casing Resistivity Problem)

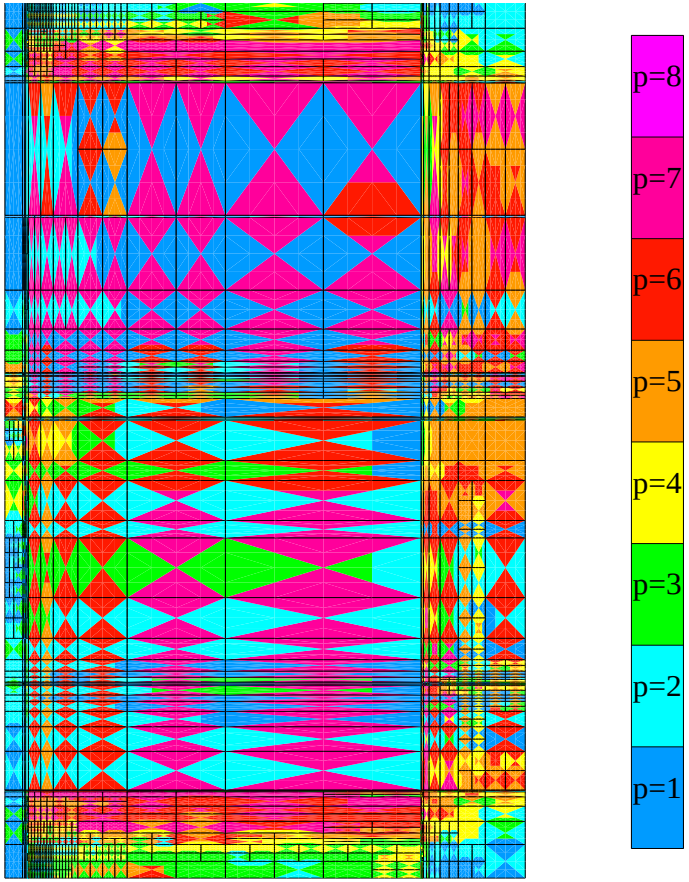

We vary locally the element size h and the polynomial order of approximation p throughout the grid.

Optimal grids are automatically generated by the computer.

The self-adaptive goal-oriented hp-FEM provides exponential convergence rates in terms of the CPU time vs. the error in a user prescribed quantity of interest.

NUMERICAL RESULTS: VERIFICATION

Three Model Problems

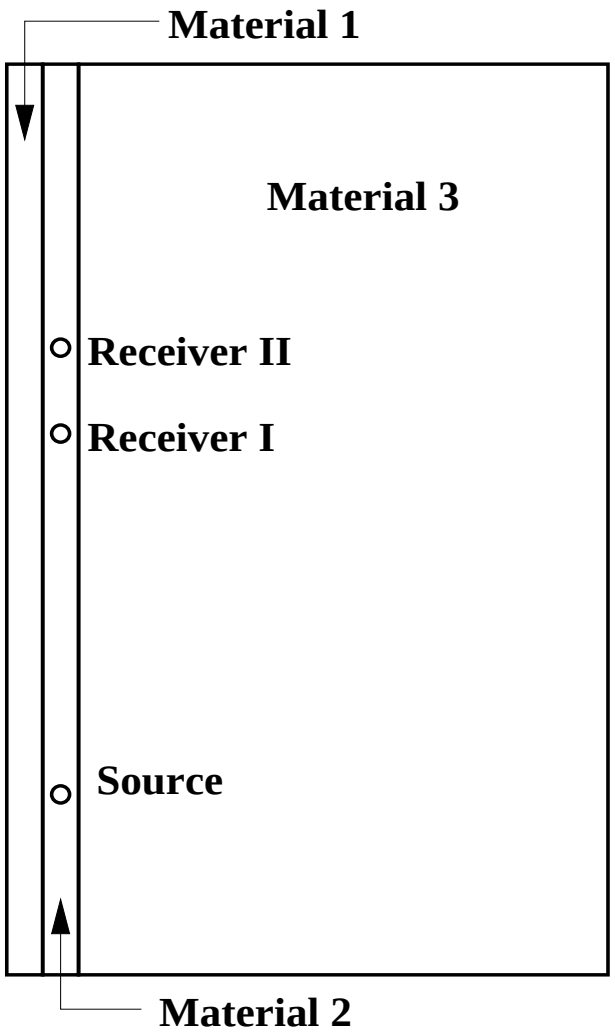

Problem I **(Uniform Materials)**

Material 1: 1 Ω−m
Material 2: 1 Ω−m
Material 3: 1 Ω−m

Problem II

Material 1: 0.00001 Ω−m
Material 2: 10 Ω−m
Material 3: 1 Ω−m

Problem III

Material 1: 10000 Ω−m
Material 2: 0.2 Ω−m
Material 3: 1 Ω−m

NUMERICAL RESULTS: VERIFICATION

Three Model Problems (DC)

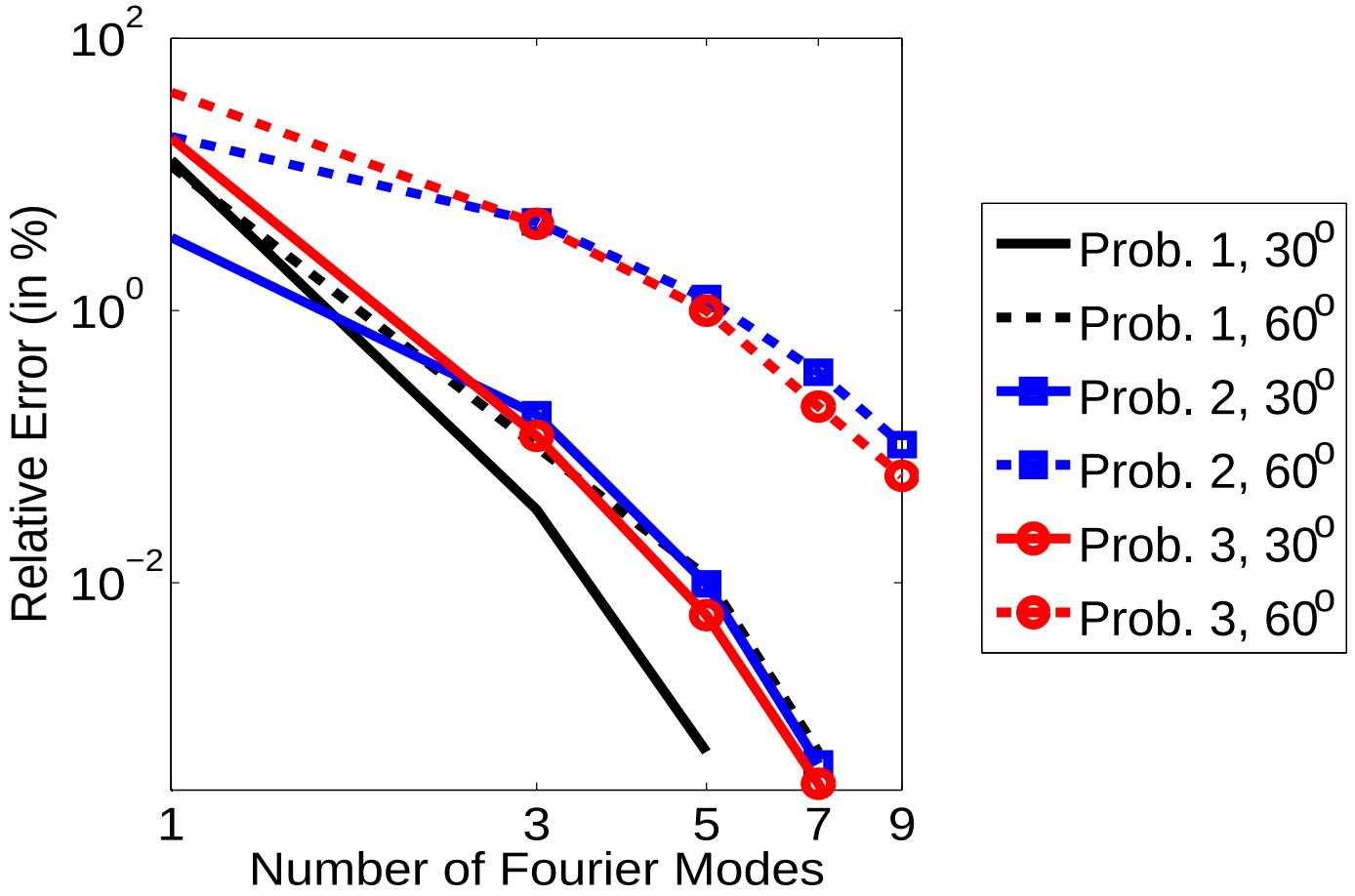

Exponential Convergence in terms of the Number of Fourier Modes

NUMERICAL RESULTS: DC RESULTS

Simulation of Through Casing Resistivity Measurements

Casing resistivity: $10^{-5} - 10^{-7} \Omega \cdot$ m

Casing thickness: 0.0127 m

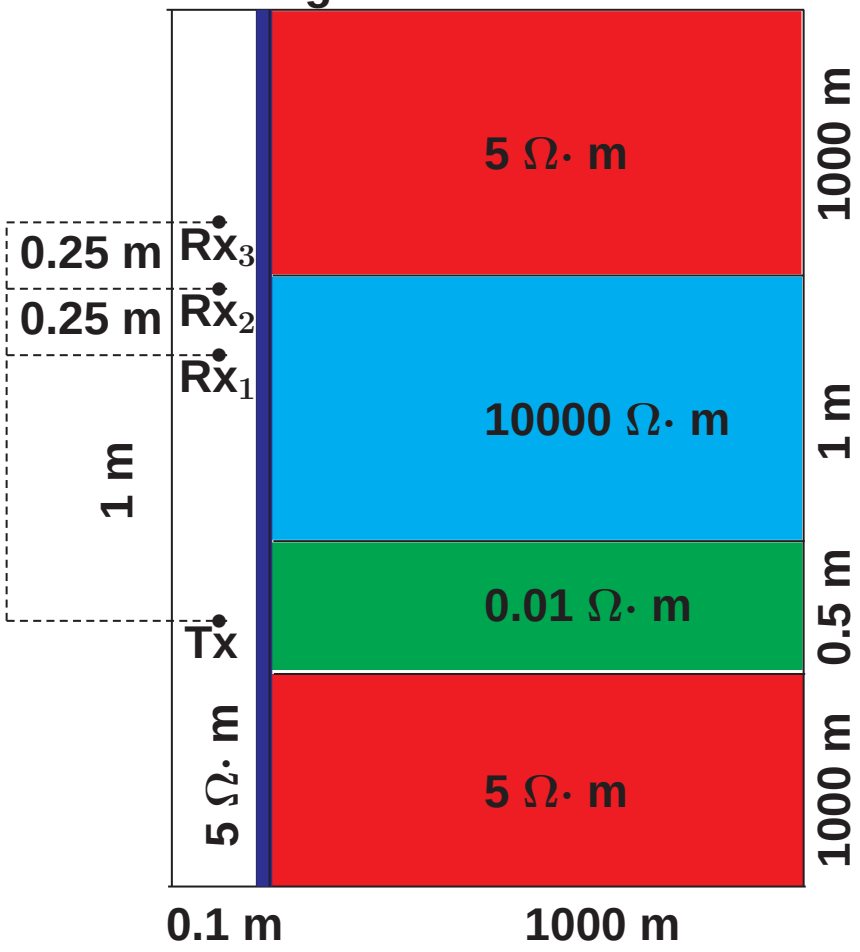

Left Figure:
- Axial-symmetric model
- One current electrode (emitter)
- Three voltage electrodes (collectors)

Objective:
- Compute second diff. of potential for various depth angles and possibly with water invasion

Method of solution:
- Fourier series expansion + change of coordinates + 2D goal-oriented hp-FEM

NUMERICAL RESULTS: DC RESULTS

Simulation of Through Casing Resistivity Measurements

Algorithm (Case) Number	I	II	III	IV	V	VI	VII	VIII
1 Fourier mode used for adaptivity	X	X	X	X				
5 Fourier modes used for adaptivity					X	X	X	X
Final hp-grid NOT p-enriched	X		X		X		X	
Final hp-grid globally p-enriched		X		X		X		X
9 Fourier modes used for the final solution	X	X			X	X		
15 Fourier modes used for the final solution			X	X			X	X

Different algorithms provide different levels of accuracy

NUMERICAL RESULTS: DC RESULTS

Through Casing Resistivity Measurements (60-Degree Deviated Well)

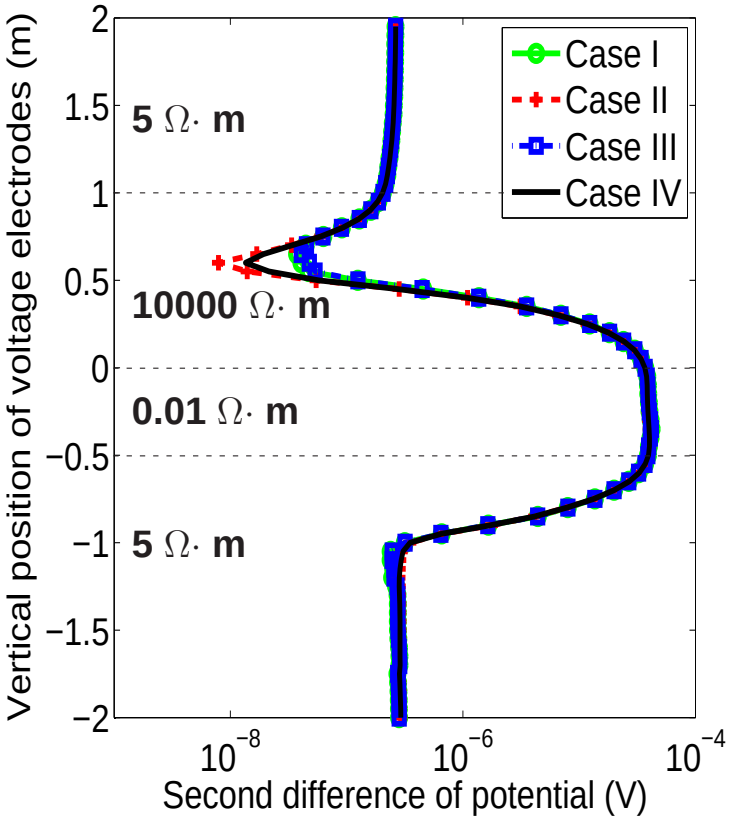

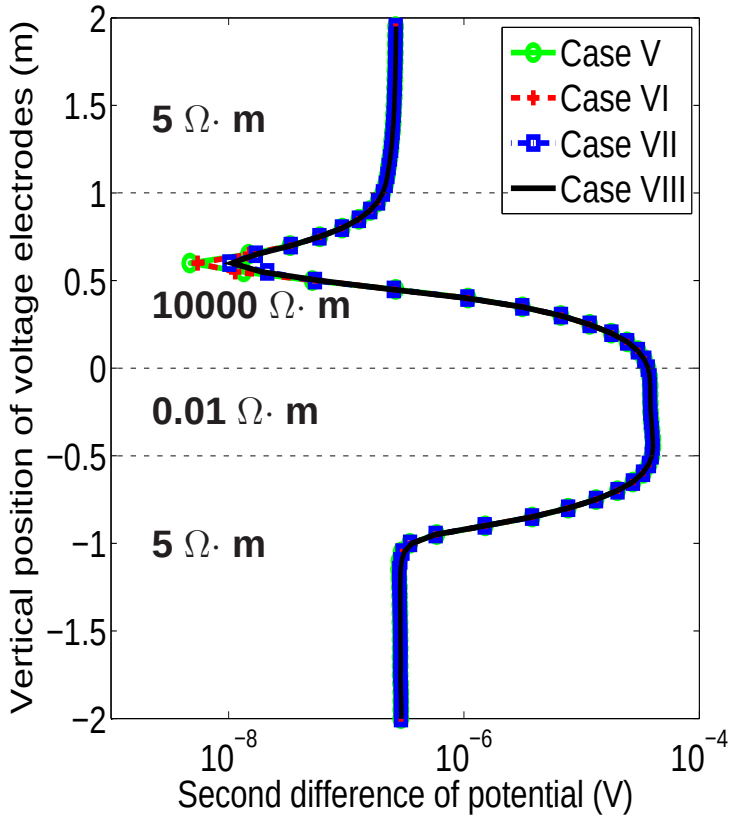

Case Number	I	II	III	IV	V	VI	VII	VIII
Total Time (minutes)	21'	40'	39'	109'	244'	290'	286'	432'

NUMERICAL RESULTS: DC RESULTS

Through Casing Resistivity Measurements (60-Degree Deviated Well)

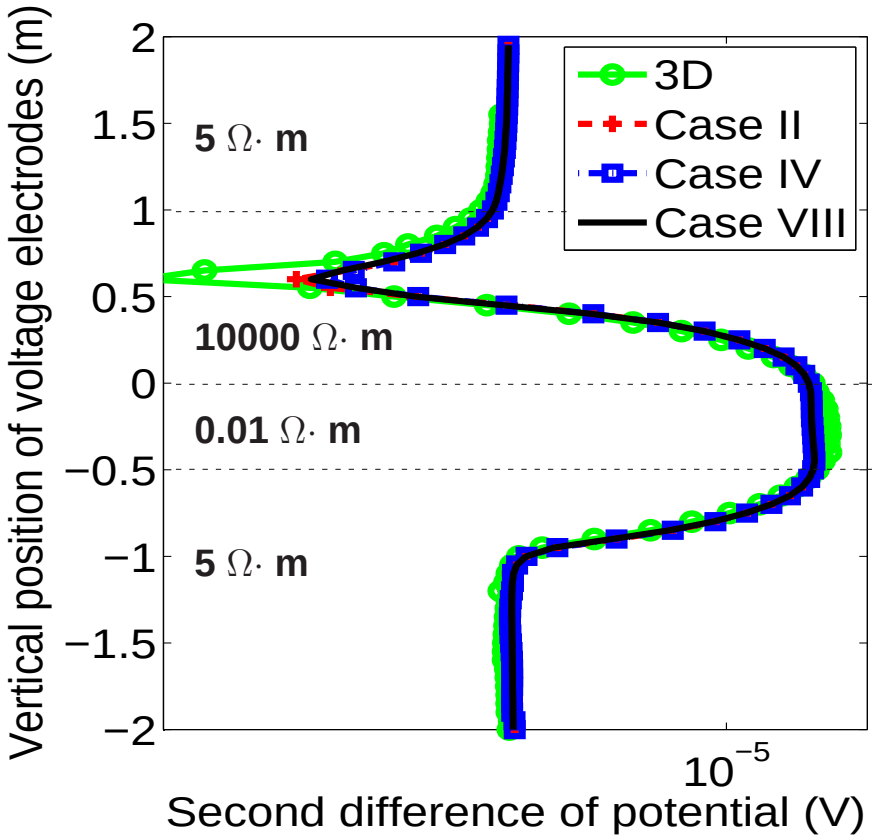

Results with the new methodology seem more accurate than those obtained with the 3D software. In addition, with the new methology we reduce the CPU time from several days to two hours.

NUMERICAL RESULTS: DC RESULTS

Through Casing Resistivity Measurements (Casing Conductivity)

Casing Resistivity=$10^{-5}\Omega\cdot$ m **Casing Resistivity=$2.3 \times 10^{-7}\Omega\cdot$ m**

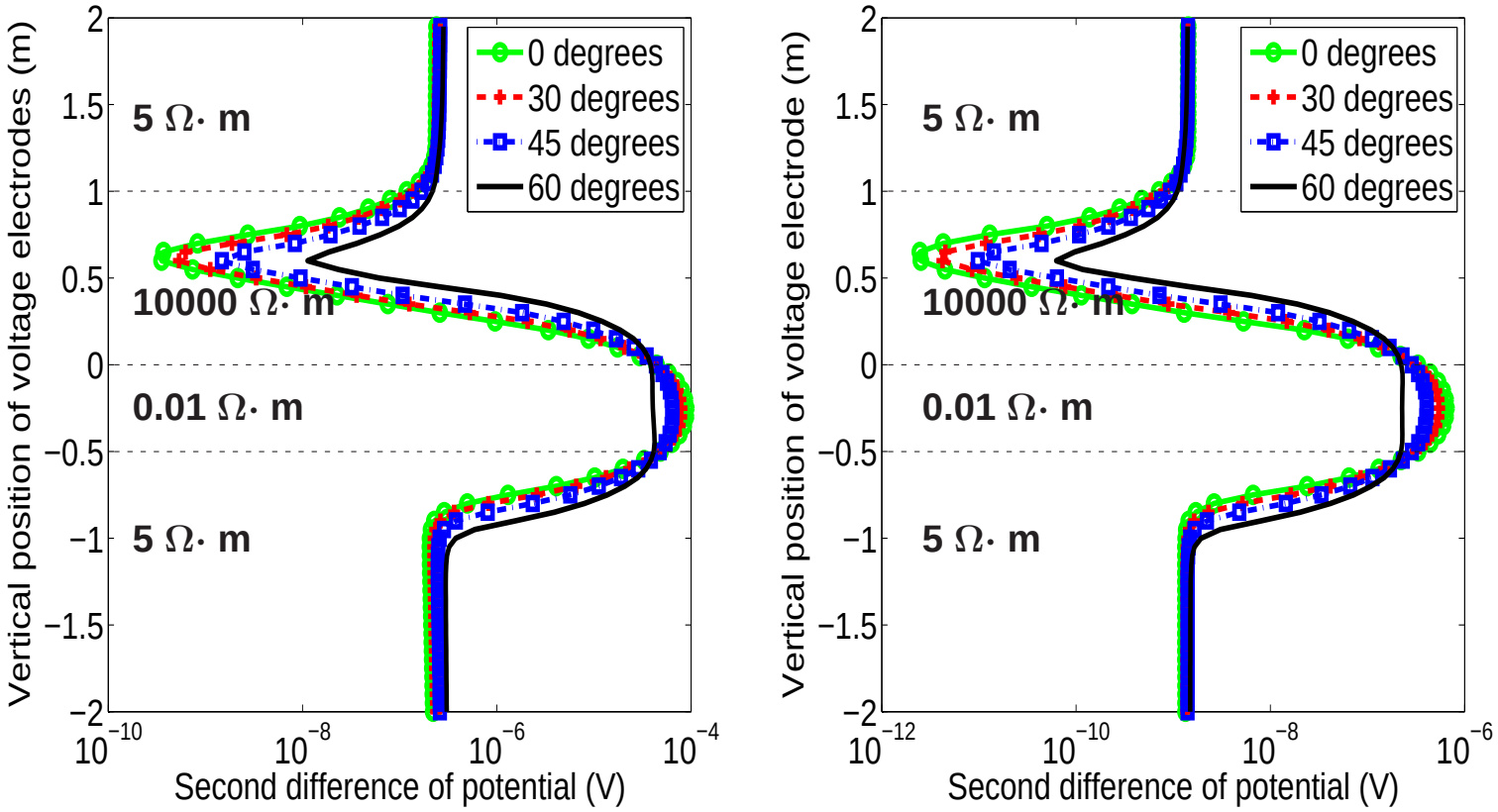

Qualitatively, results for various casing conductivities are similar even for deviated wells.

NUMERICAL RESULTS: DC RESULTS

Through Casing Resistivity Measurements (Invasion)

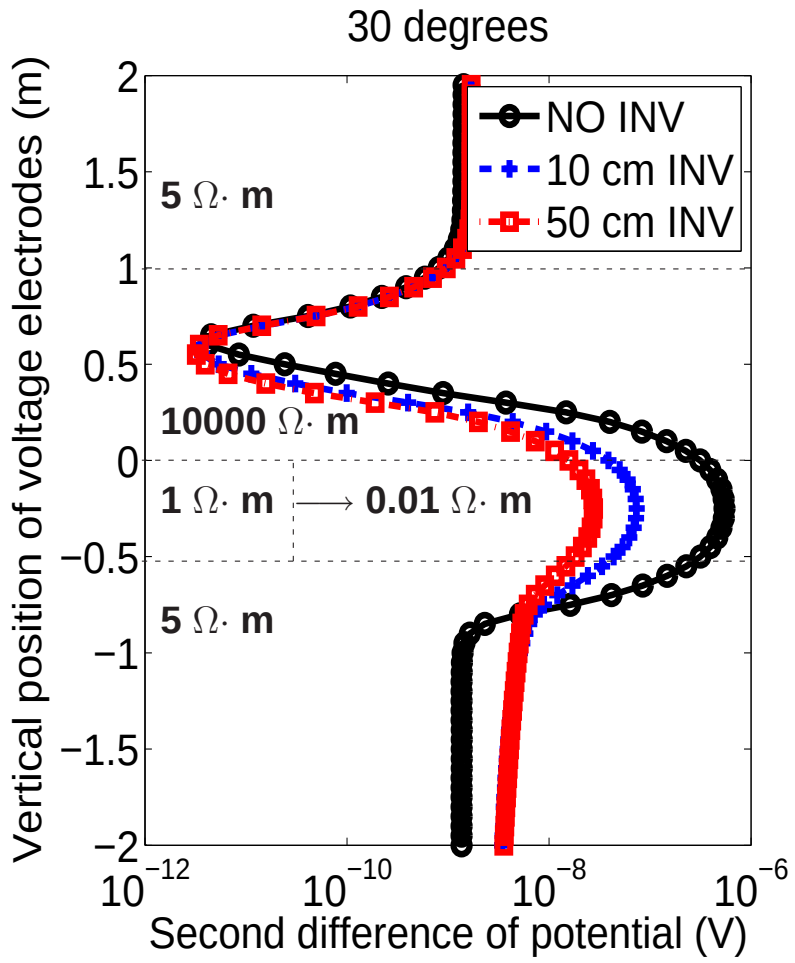

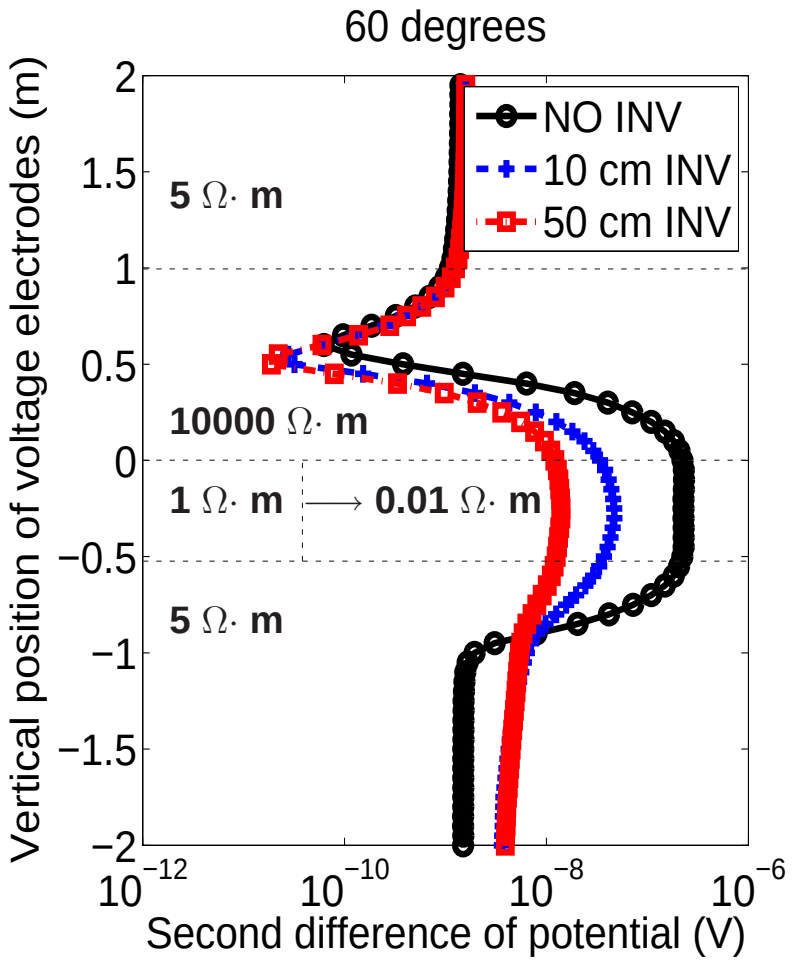

NUMERICAL RESULTS: DC RESULTS

Through Casing Resistivity Measurements (Invasion)

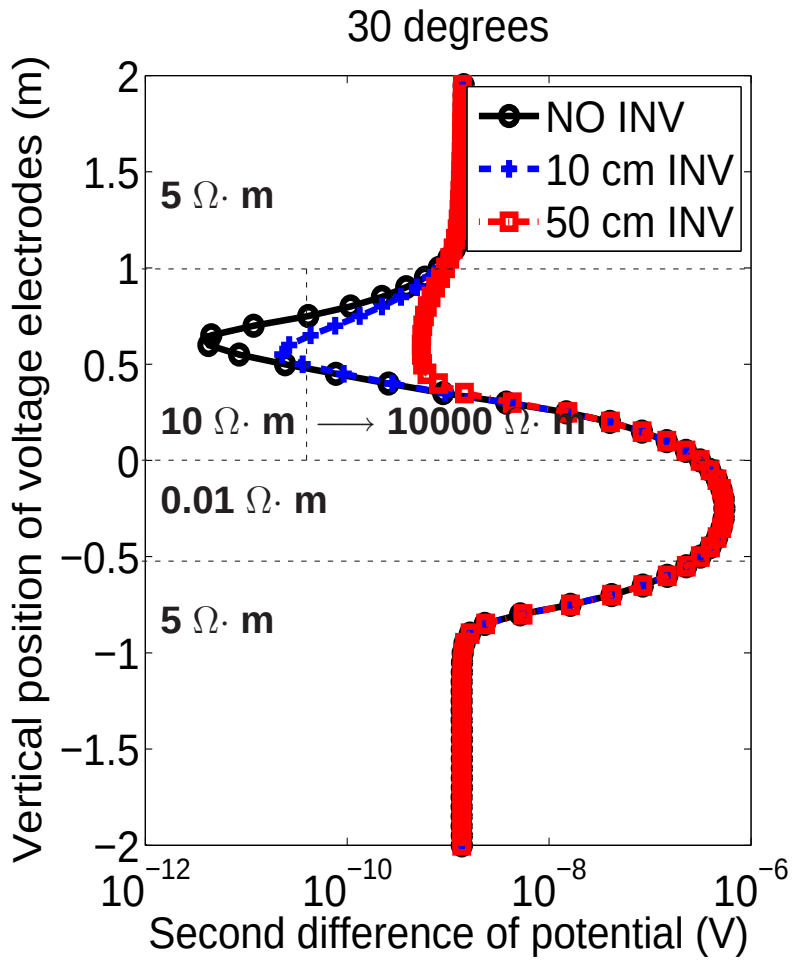

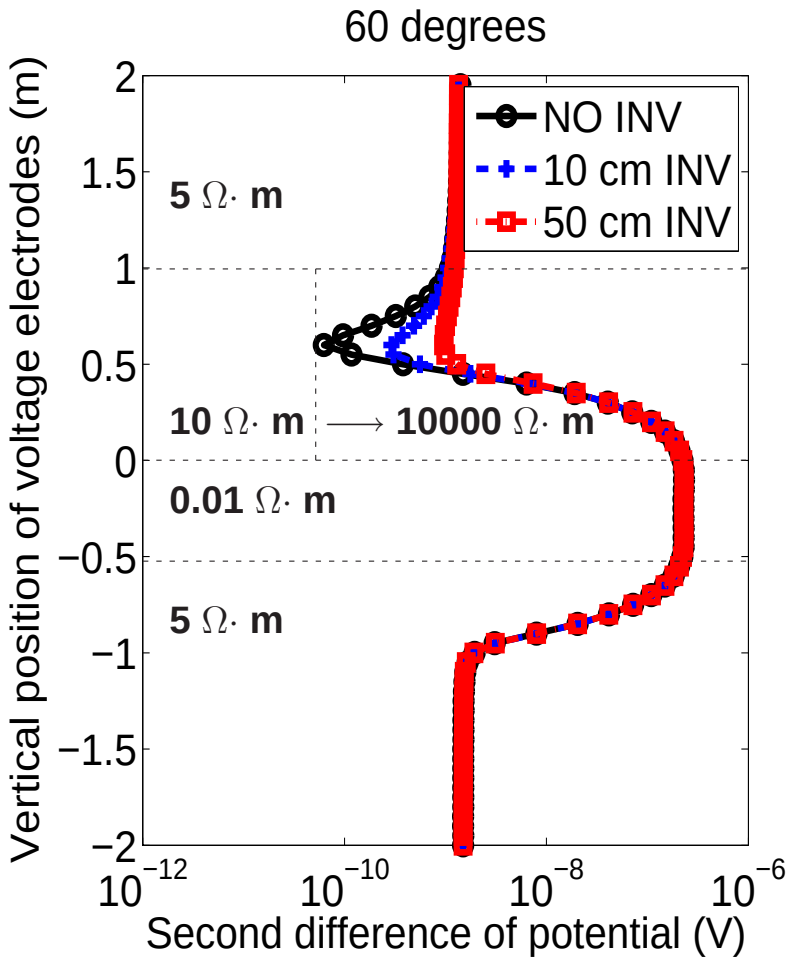

NUMERICAL RESULTS: DC LATEROLOG

- Description of Tool

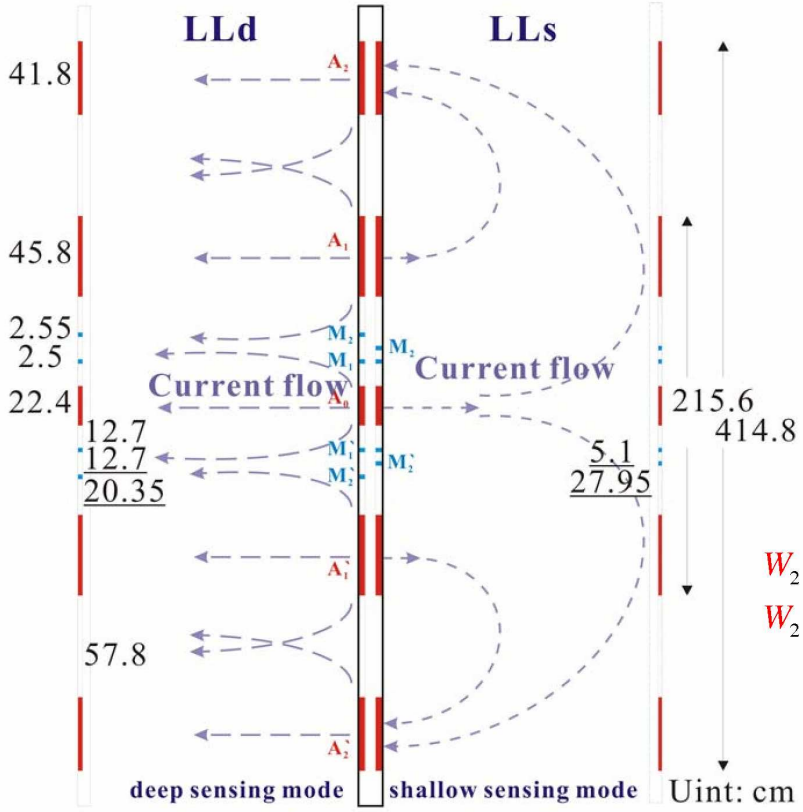

DUAL LATEROLOG - Halliburton Energy Services

- Determination of Intensities (W_j) of Bucking Currents

Focusing Conditions

$$V(M_1) = V(M_2)$$
$$V(M_{1'}) = V(M_{2'})$$

Relationships between W_j

$$W_2 = (W_1 + c), \quad W_{2'} = (W_{1'} + c) \quad for \text{ LLd}$$
$$W_2 = -(W_1 + c), \quad W_{2'} = -(W_{1'} + c) \quad for \text{ LLs}$$

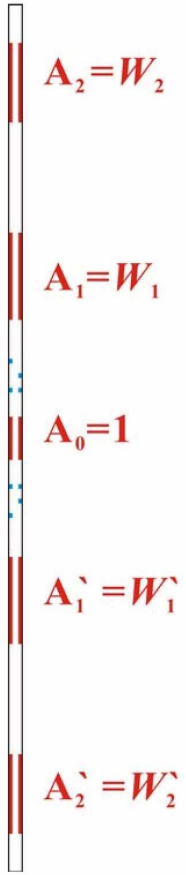

NUMERICAL RESULTS: DC LATEROLOG

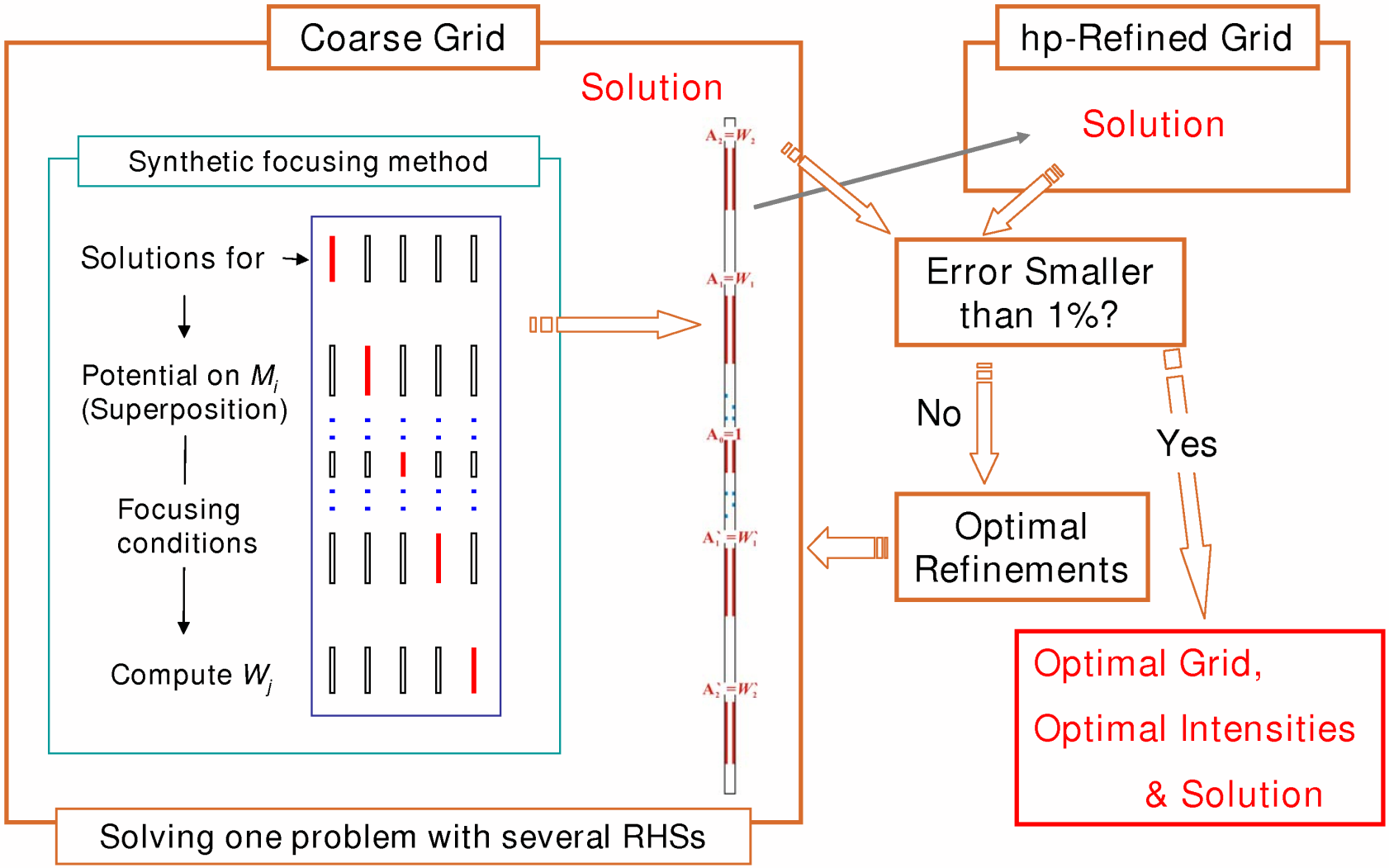

NUMERICAL RESULTS: DC LATEROLOG

Model

Using the Tool Configuration of Halliburton Energy Services' DLL

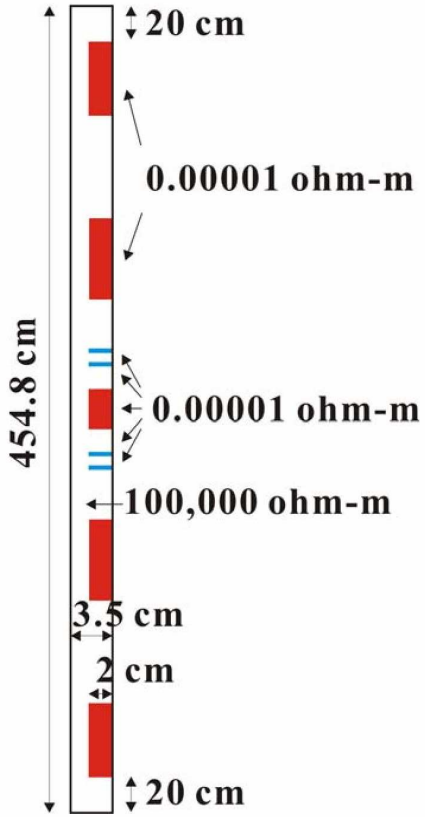

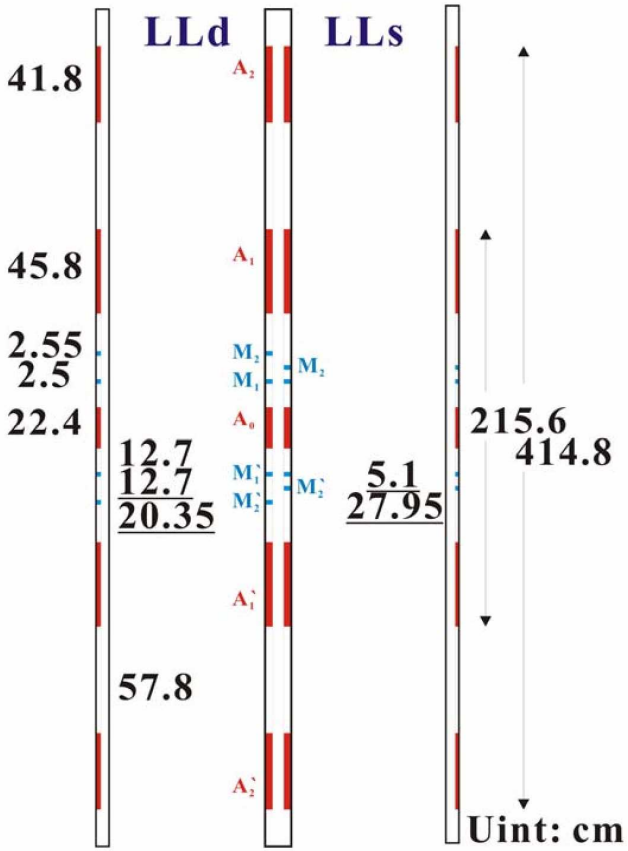

NUMERICAL RESULTS: DC LATEROLOG

θ = 0, 30 and 60 degrees

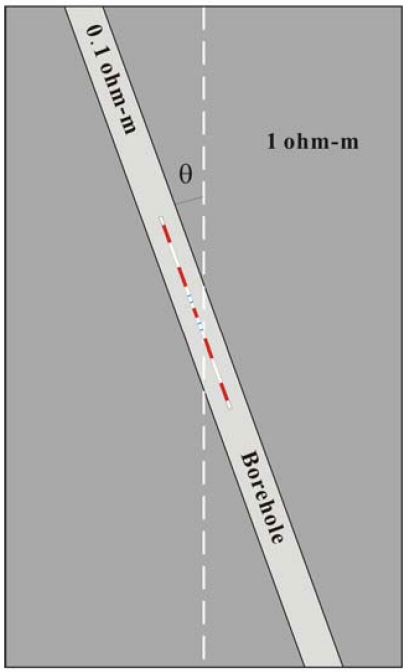

Relative errors of laterolog instruments in a homogeneous formation

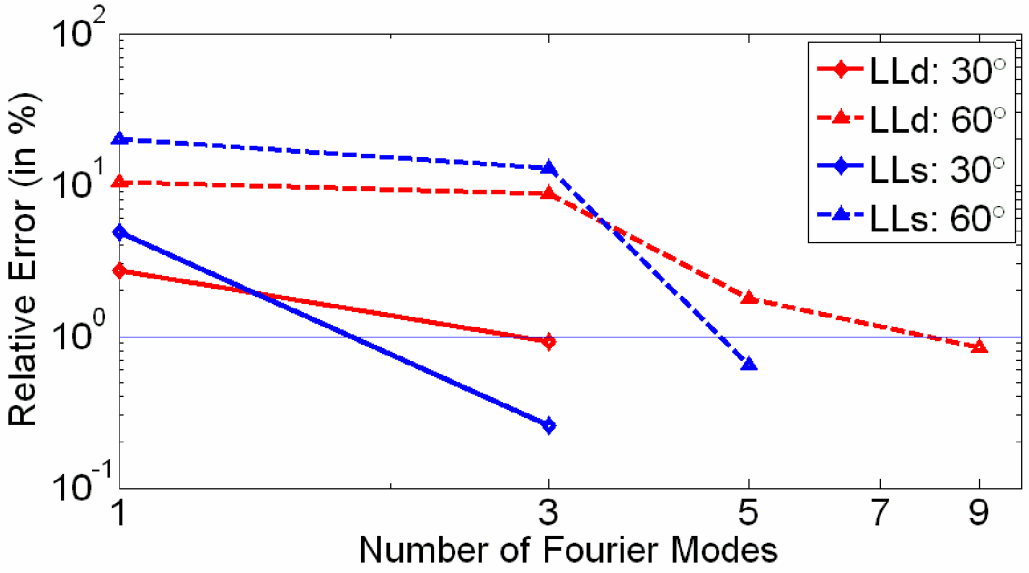

NUMERICAL RESULTS: DC LATEROLOG

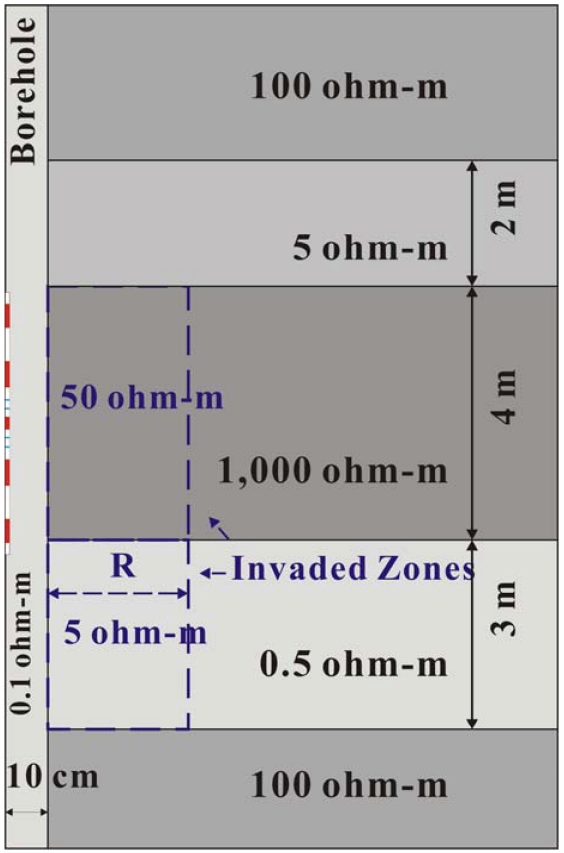

Five layers: 100, 5, 1000, 0.5
and 100 ohm-m from top to bottom

Borehole: 0.1 m in radius
0.1 ohm-m in resistivity

Invasion

Anisotropy

NUMERICAL RESULTS: DC LATEROLOG

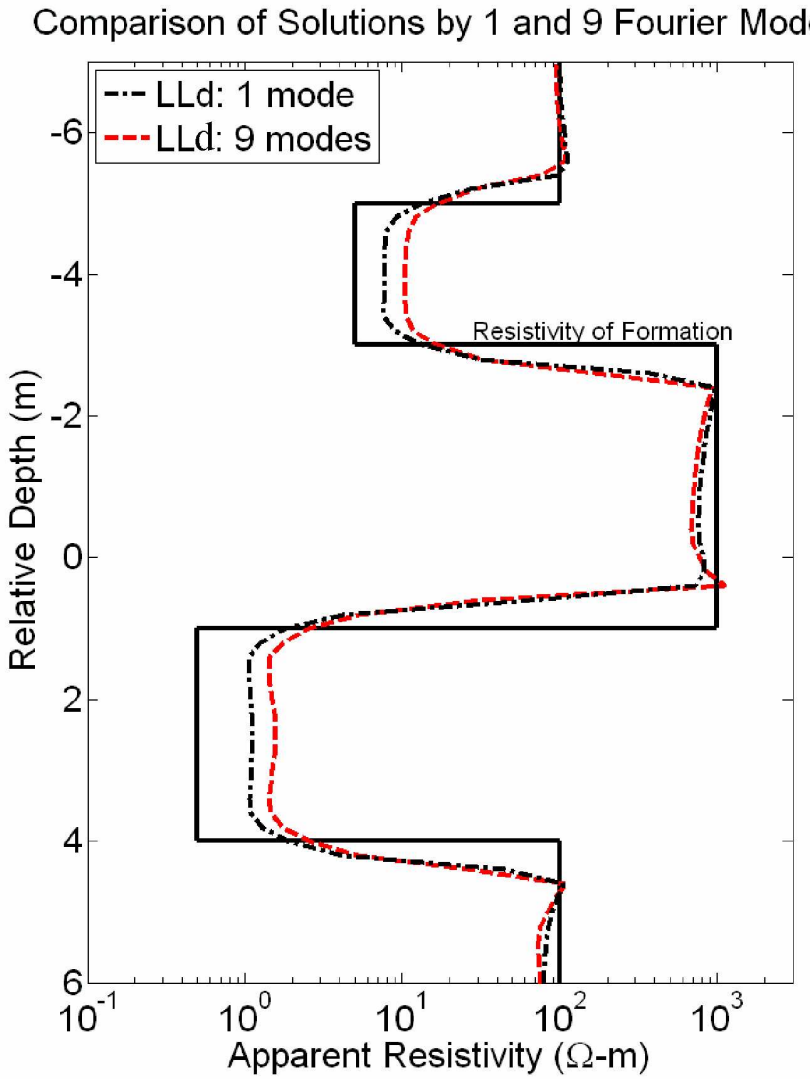

Dip angle: 45 degrees

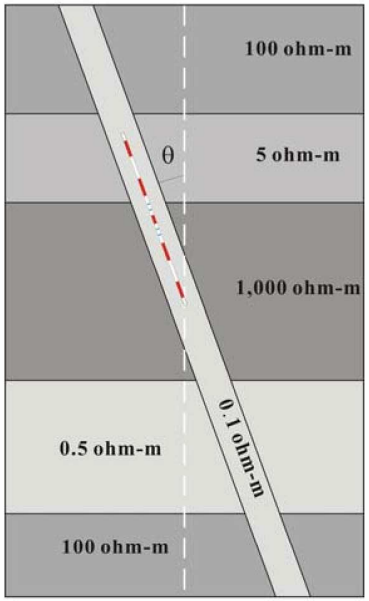

NUMERICAL RESULTS: DC LATEROLOG

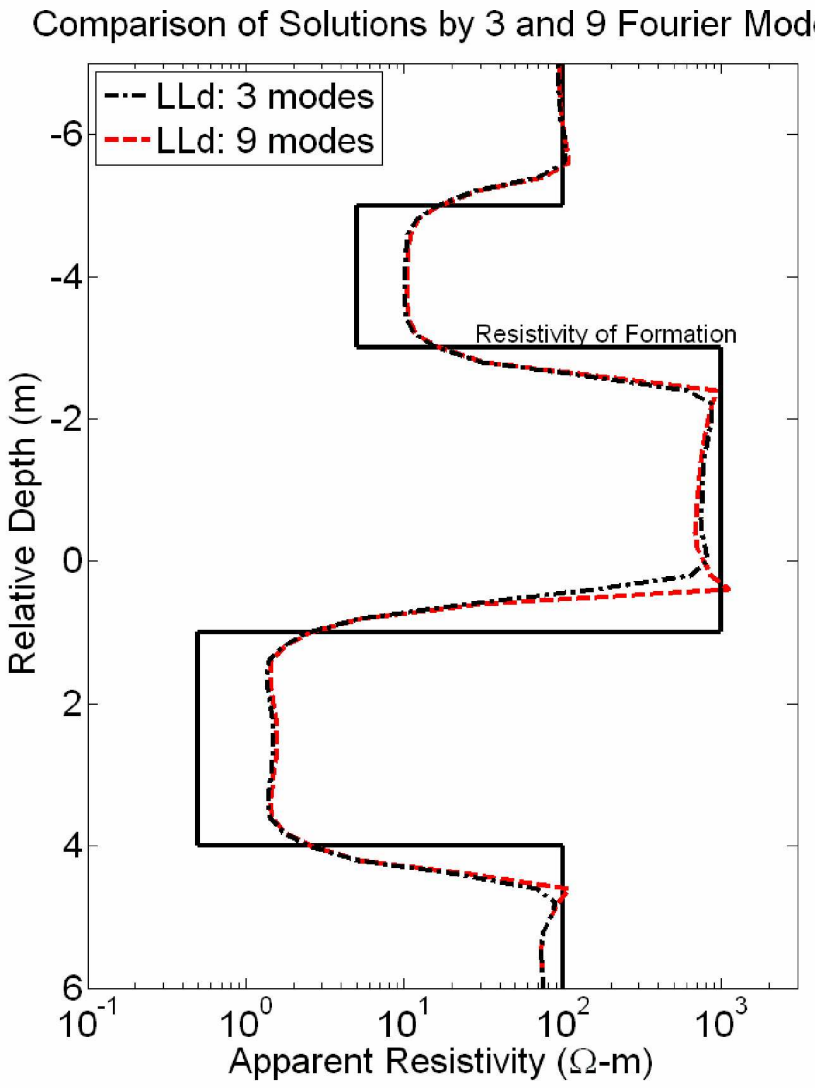

Dip angle: 45 degrees

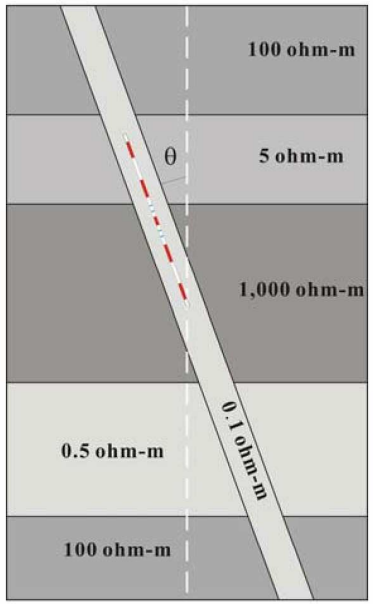

NUMERICAL RESULTS: DC LATEROLOG

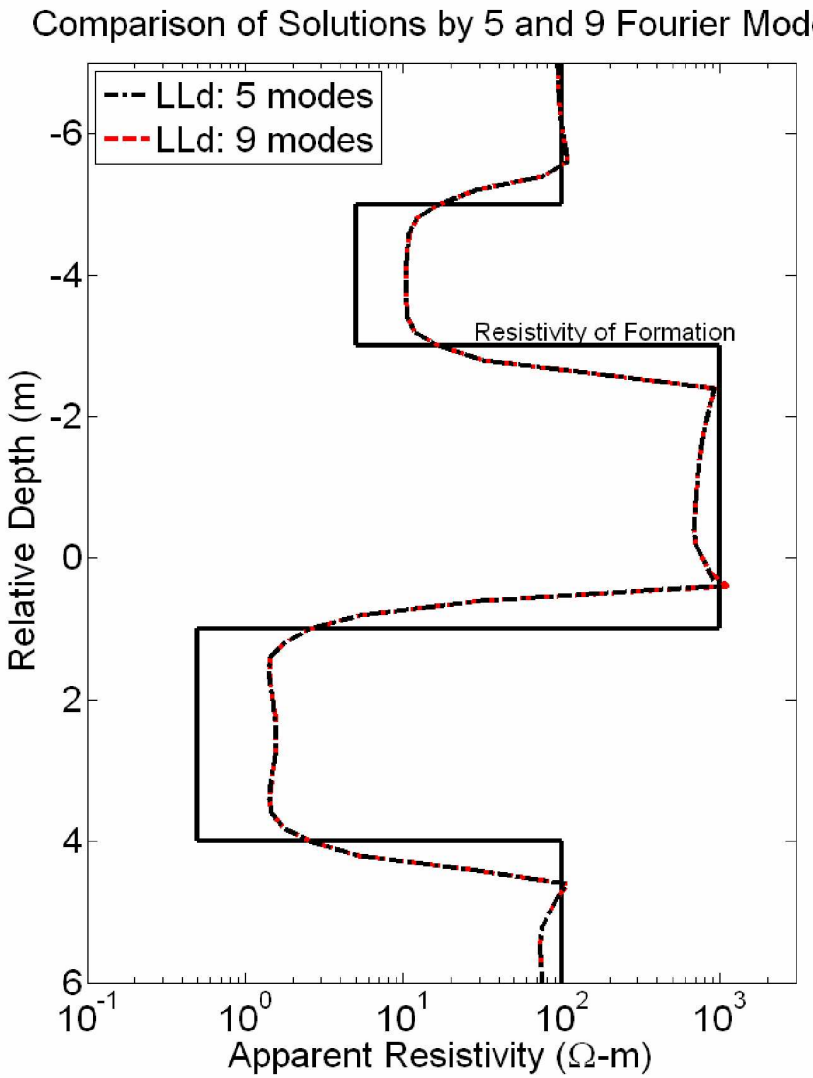

Dip angle: 45 degrees

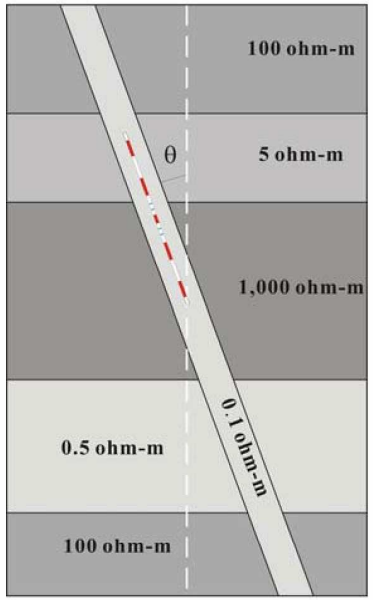

NUMERICAL RESULTS: DC LATEROLOG

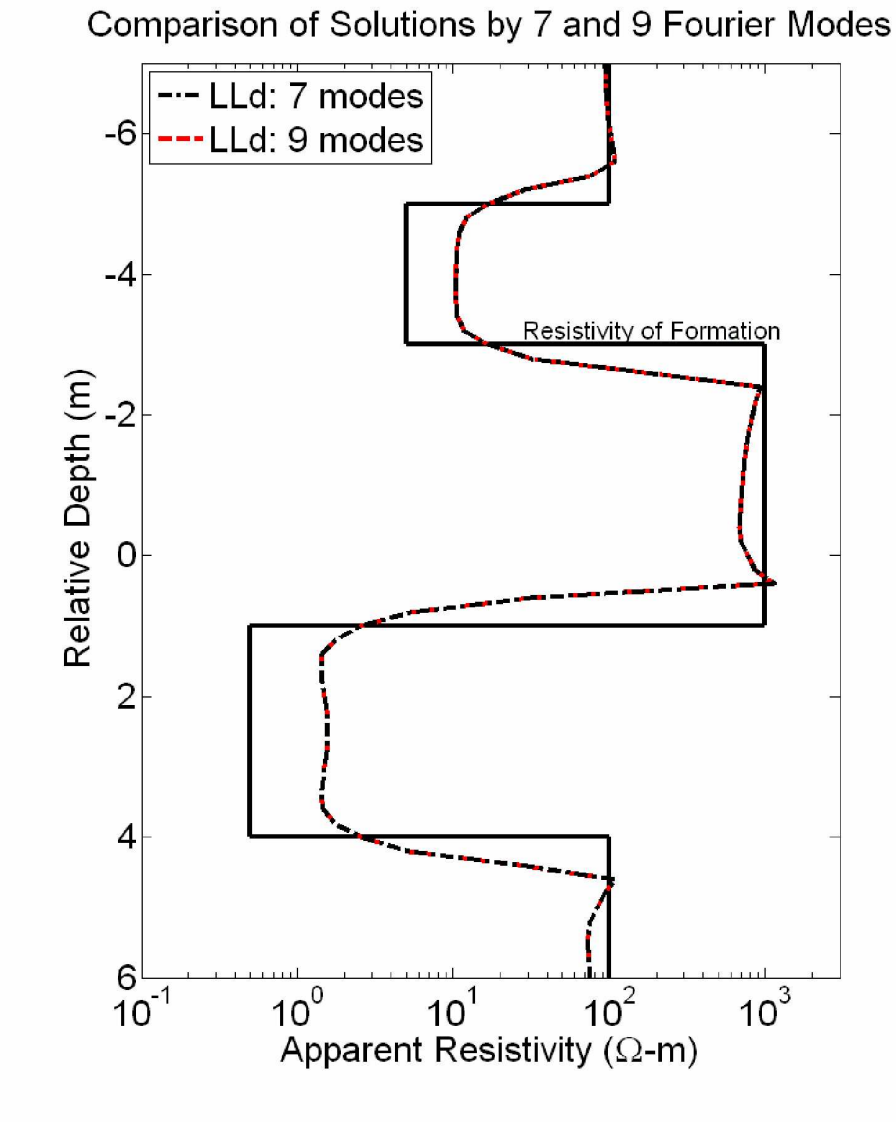

Dip angle: 45 degrees

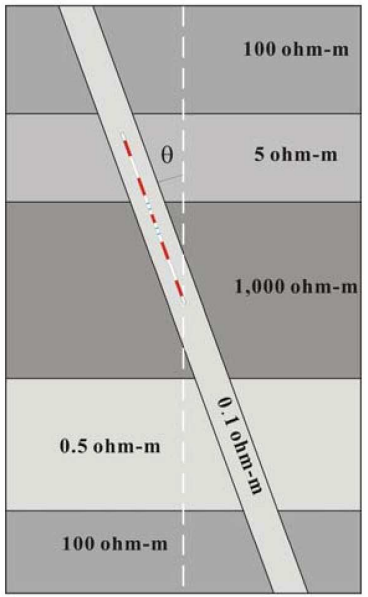

NUMERICAL RESULTS: DC LATEROLOG

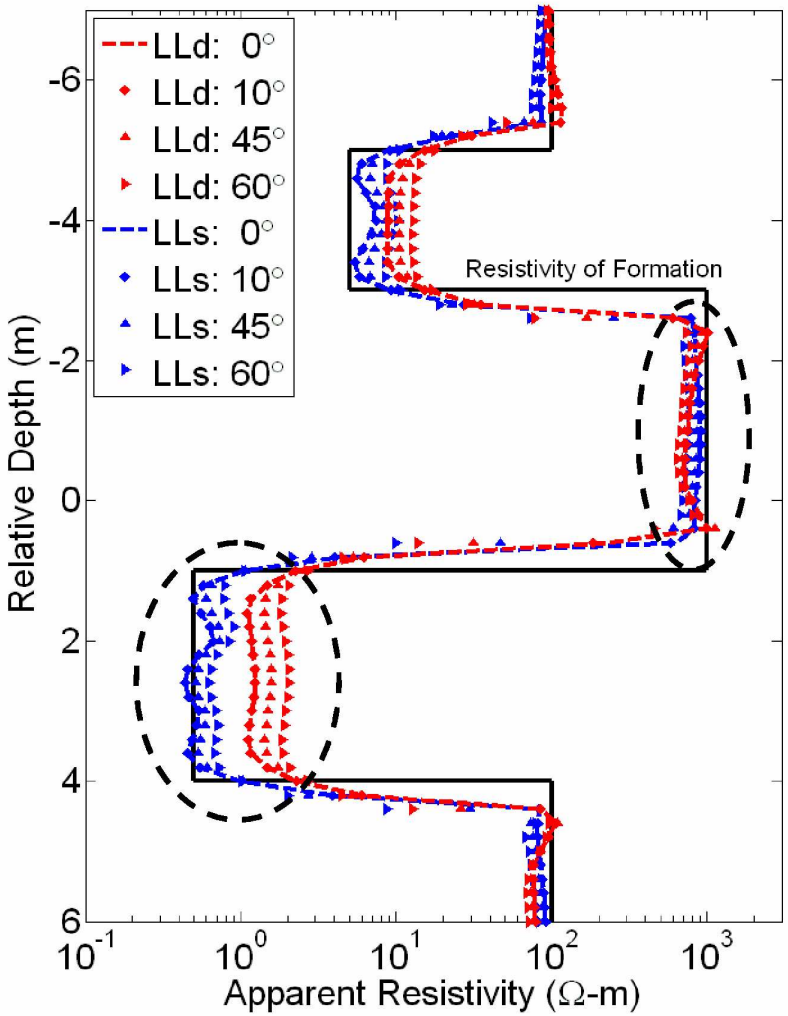

Effects of dip angle: Conductive layer ↑

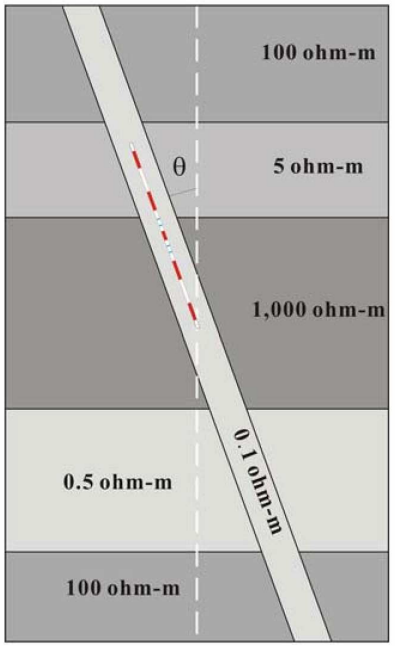

NUMERICAL RESULTS: DC LATEROLOG

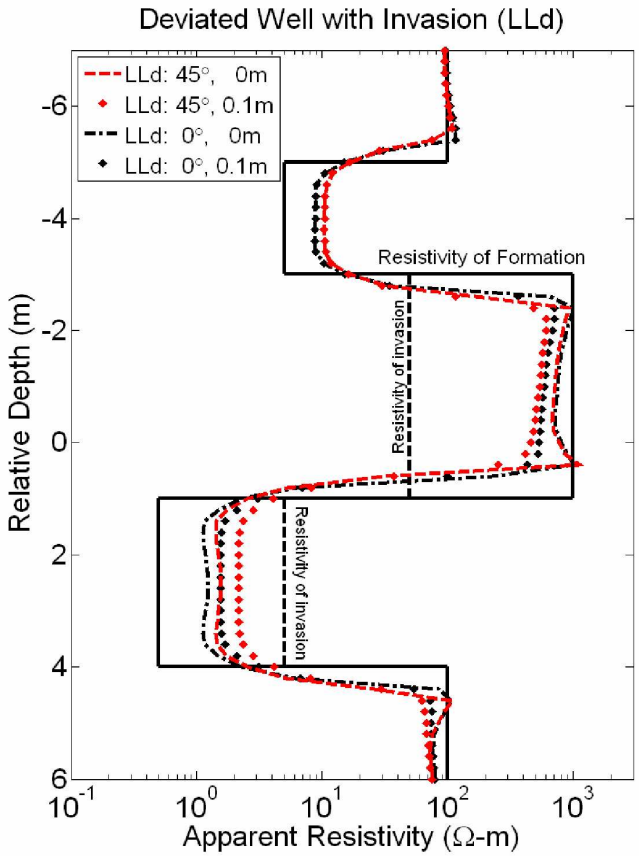

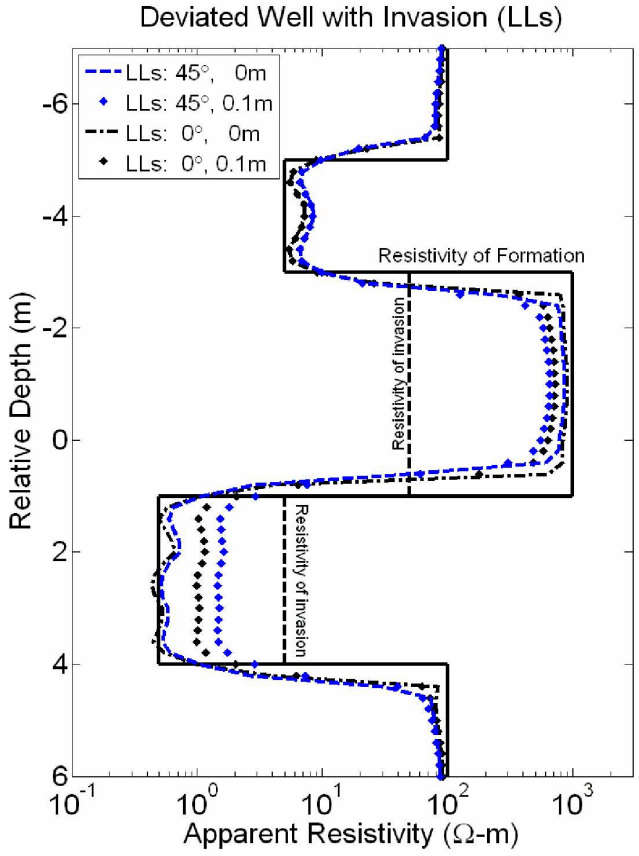

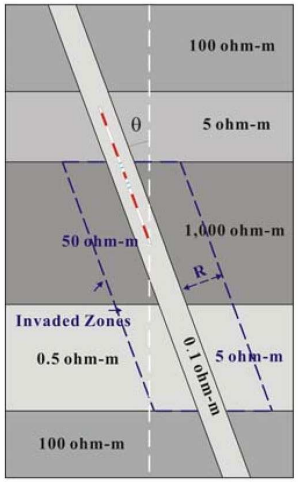

Effects of invasion to LLs: larger in a 45-degree deviated well than in a vertical well in conductive layer

NUMERICAL RESULTS: DC LATEROLOG

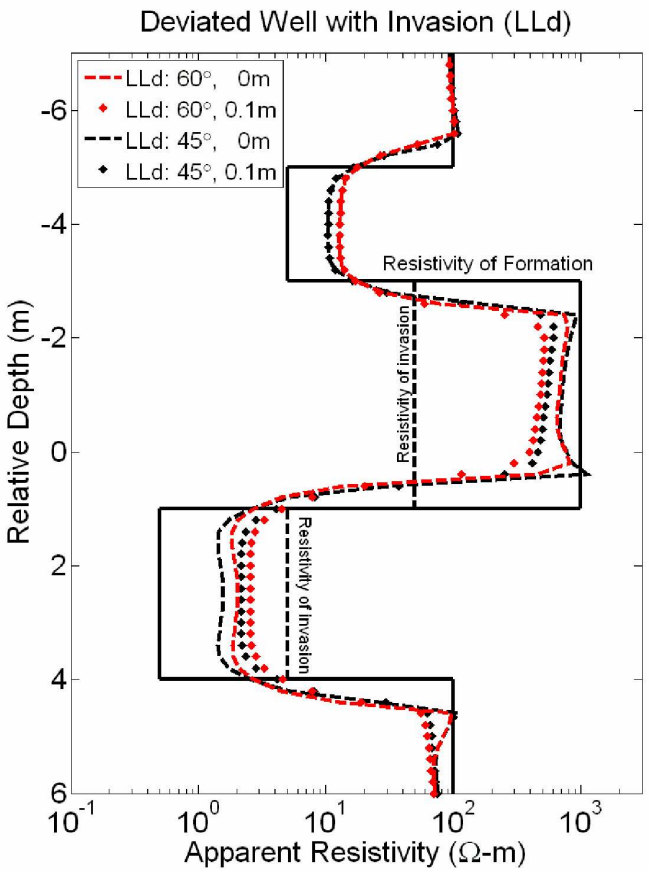

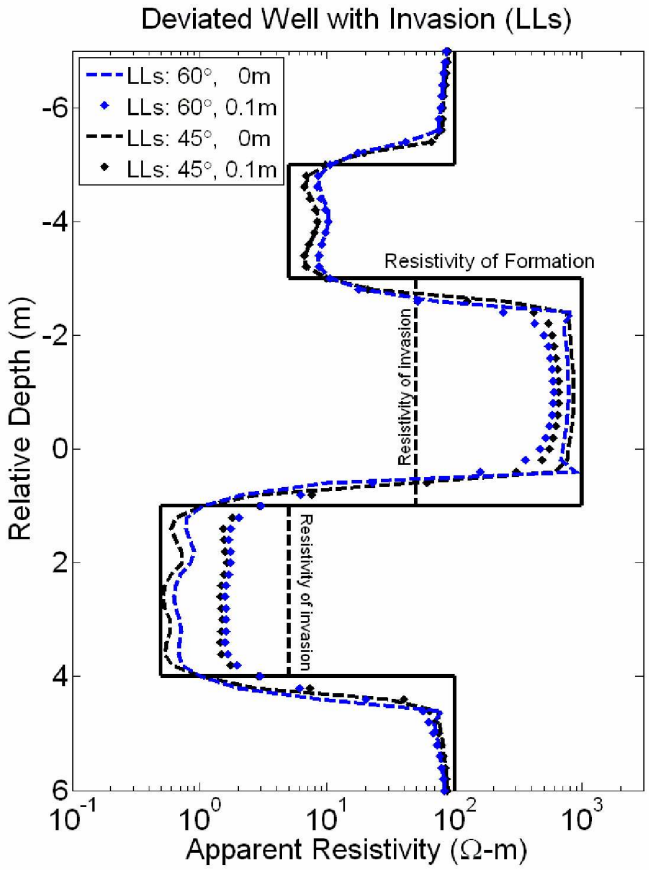

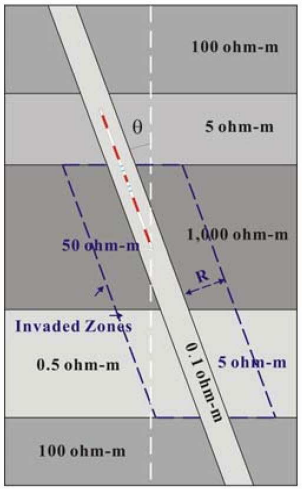

Effects of invasion to LLs: slightly smaller in a 60-degree deviated well than in a 45-degree deviated well in conductive layer

NUMERICAL RESULTS: DC LATEROLOG

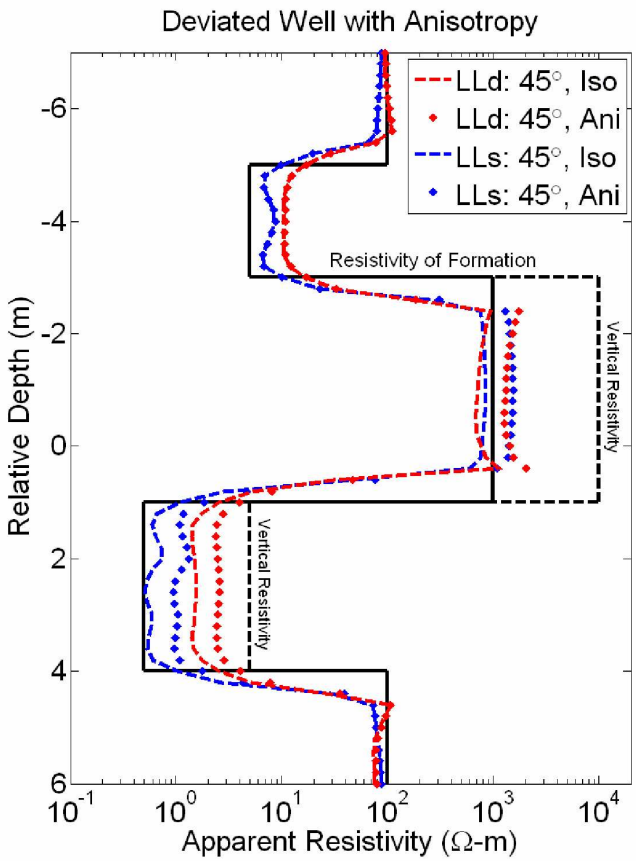

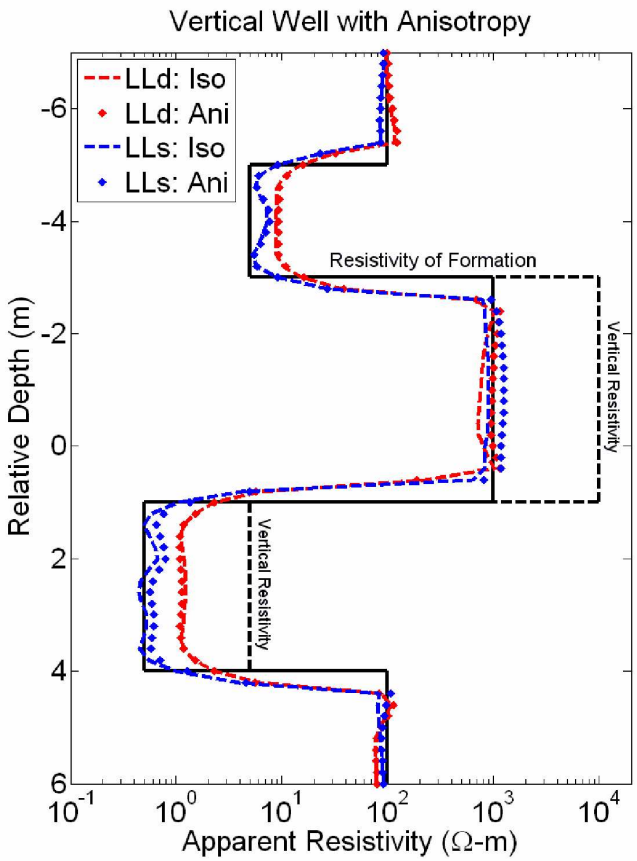

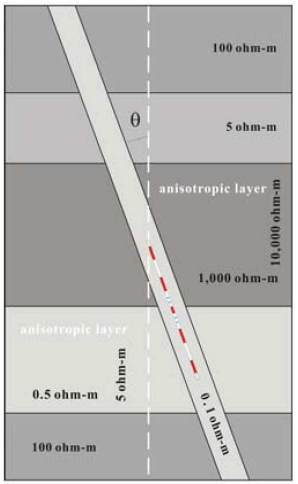

Effects of anisotropy: 45-degree deviated well ↑

NUMERICAL RESULTS: DC LATEROLOG

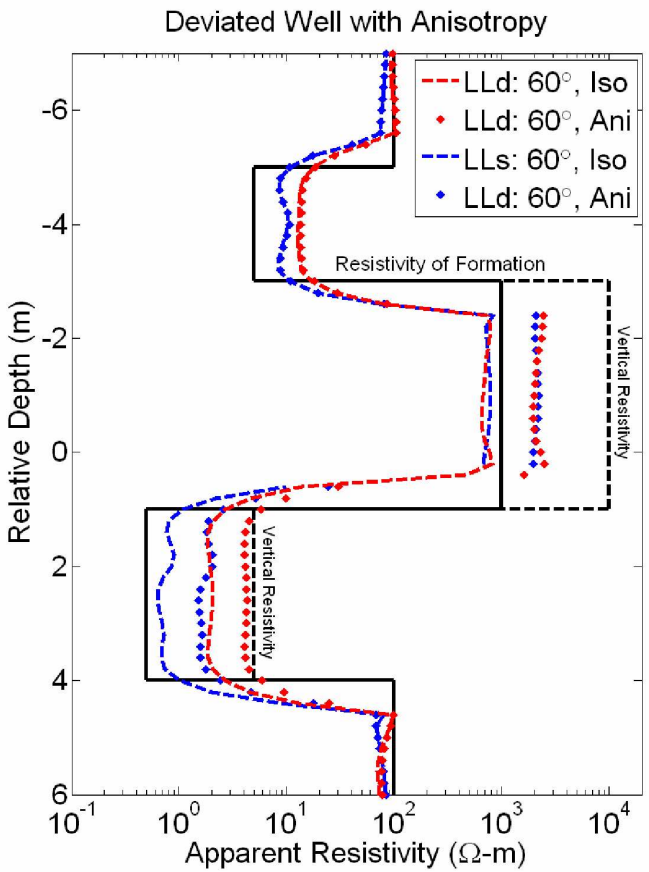

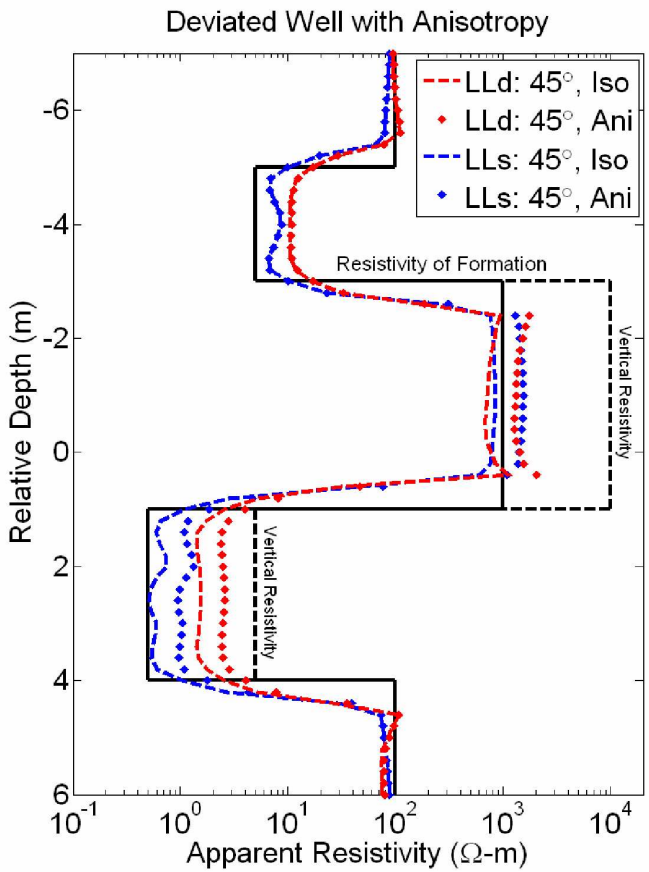

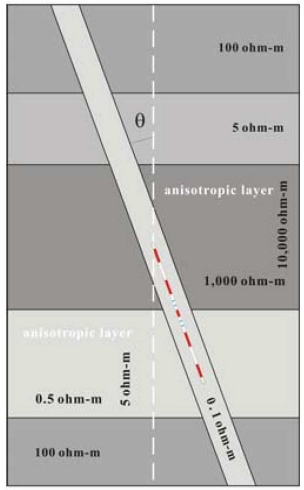

Effects of anisotropy: 60-degree deviated well ↑

NUMERICAL RESULTS: AC RESULTS

Model Problem

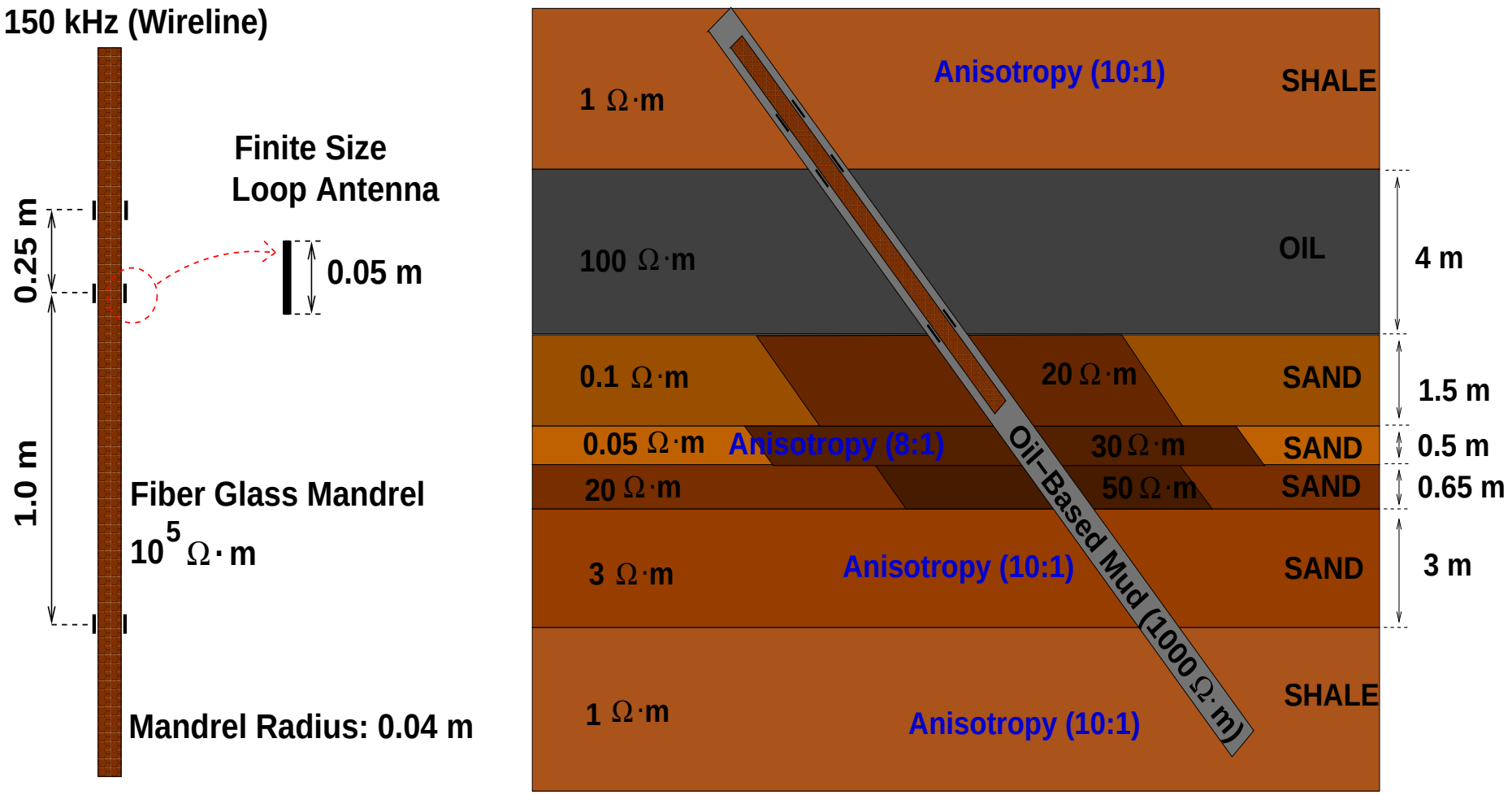

NUMERICAL RESULTS: AC RESULTS

Verification

Logging Instrument in a Homogeneous Formation

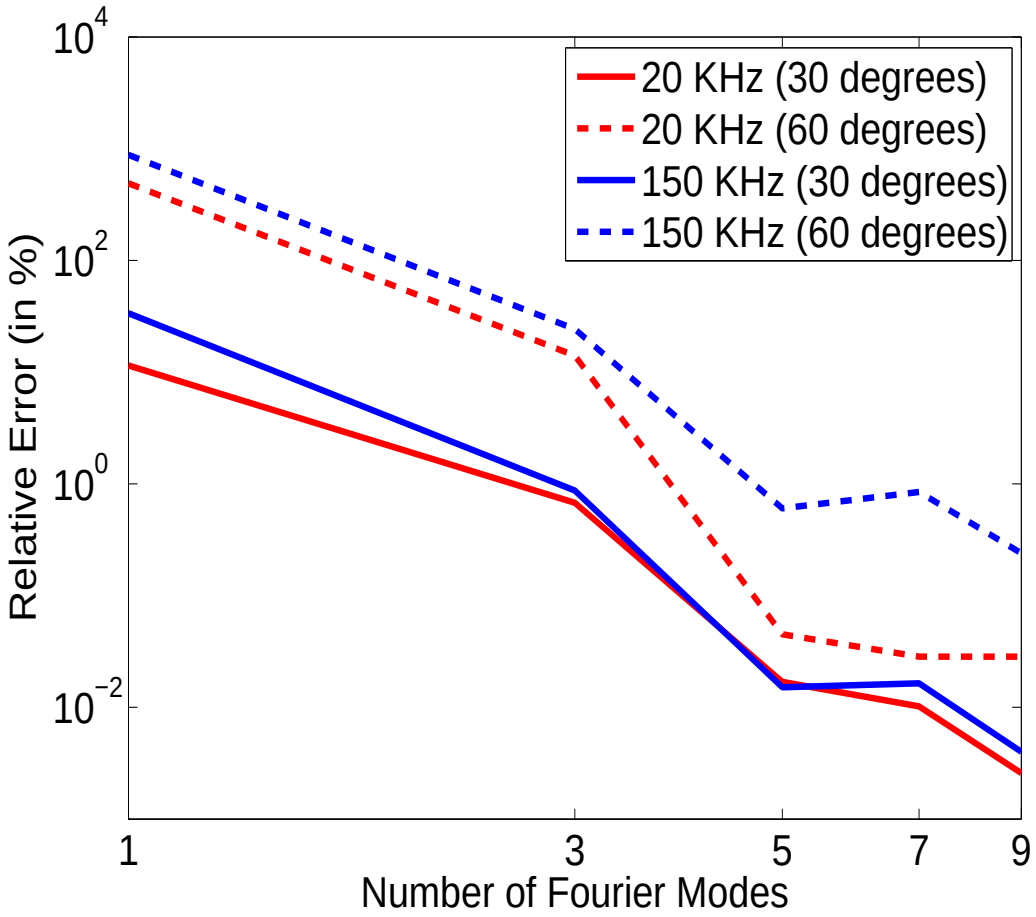

NUMERICAL RESULTS: AC RESULTS

Verification

Logging Instrument in a Homogeneous Formation

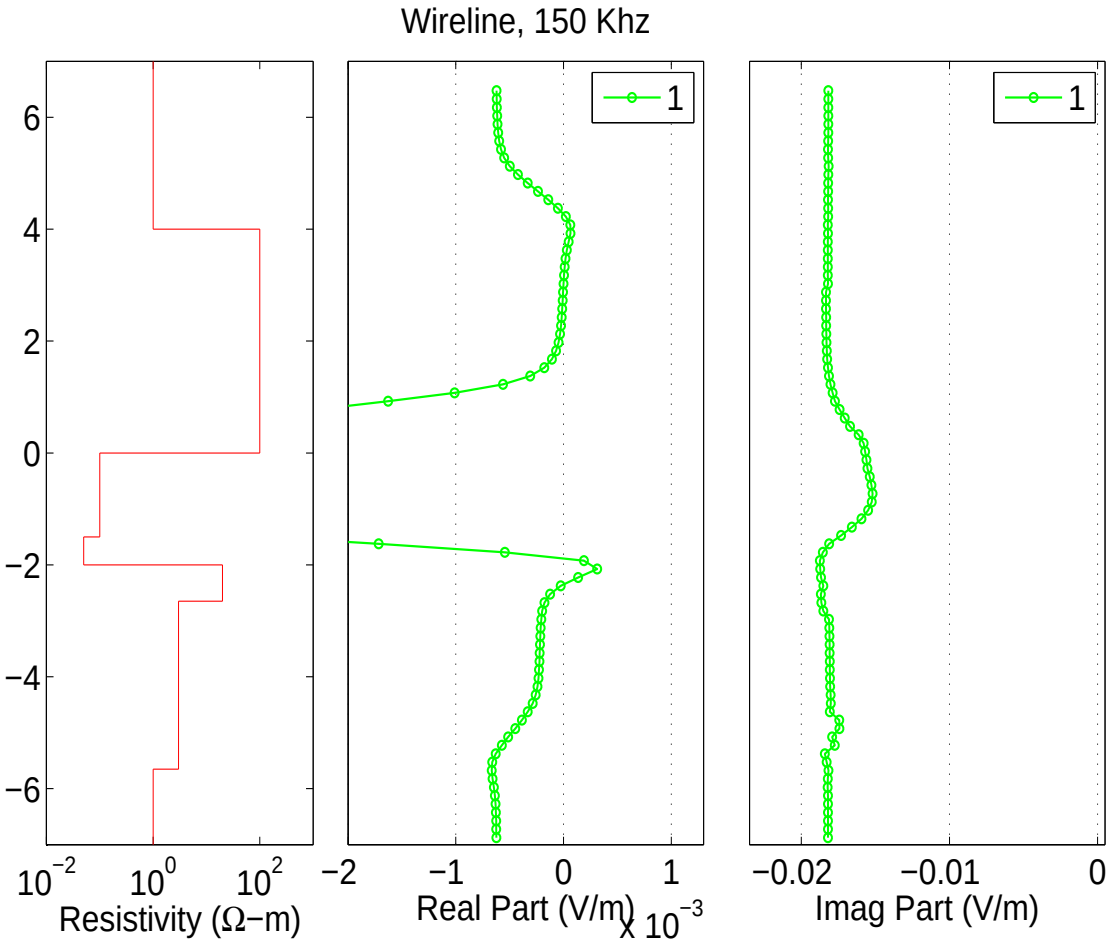

NUMERICAL RESULTS: AC RESULTS

Verification

Logging Instrument in a Homogeneous Formation

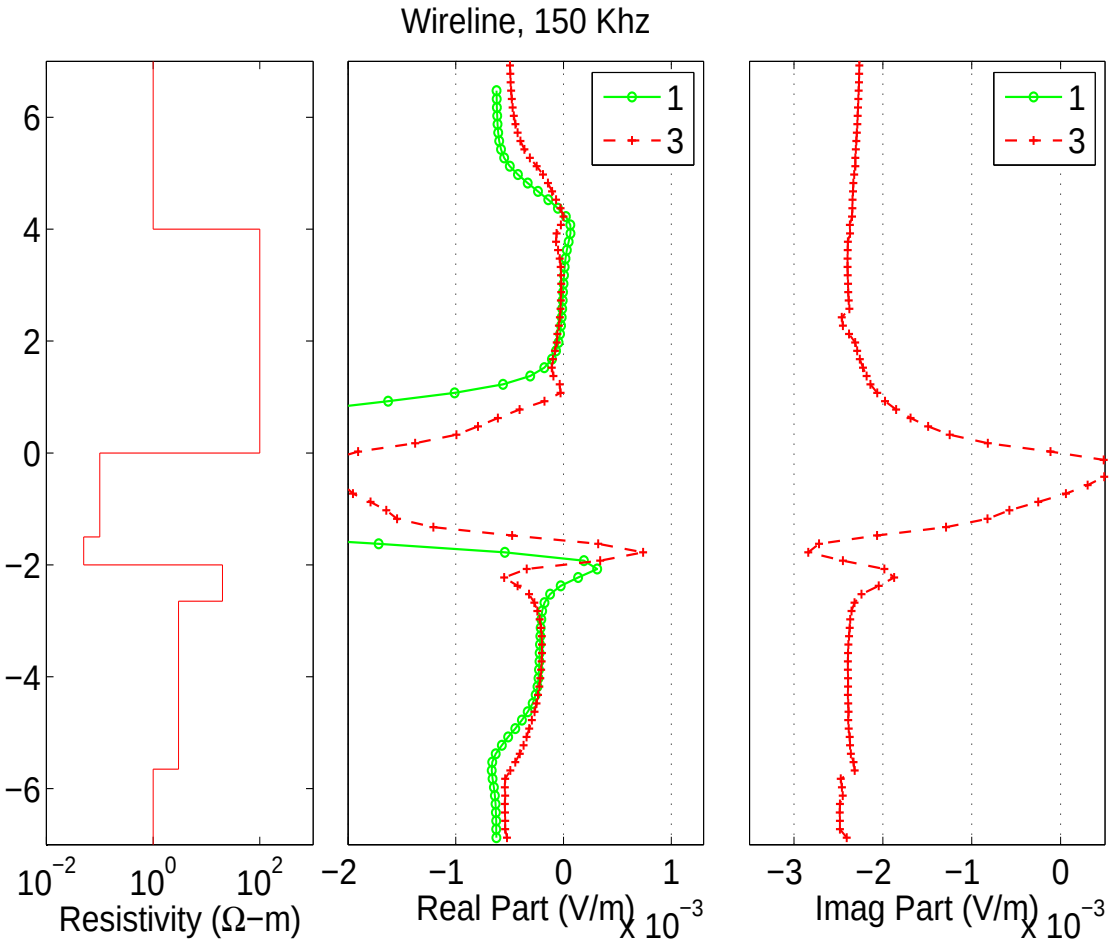

NUMERICAL RESULTS: AC RESULTS

Verification

Logging Instrument in a Homogeneous Formation

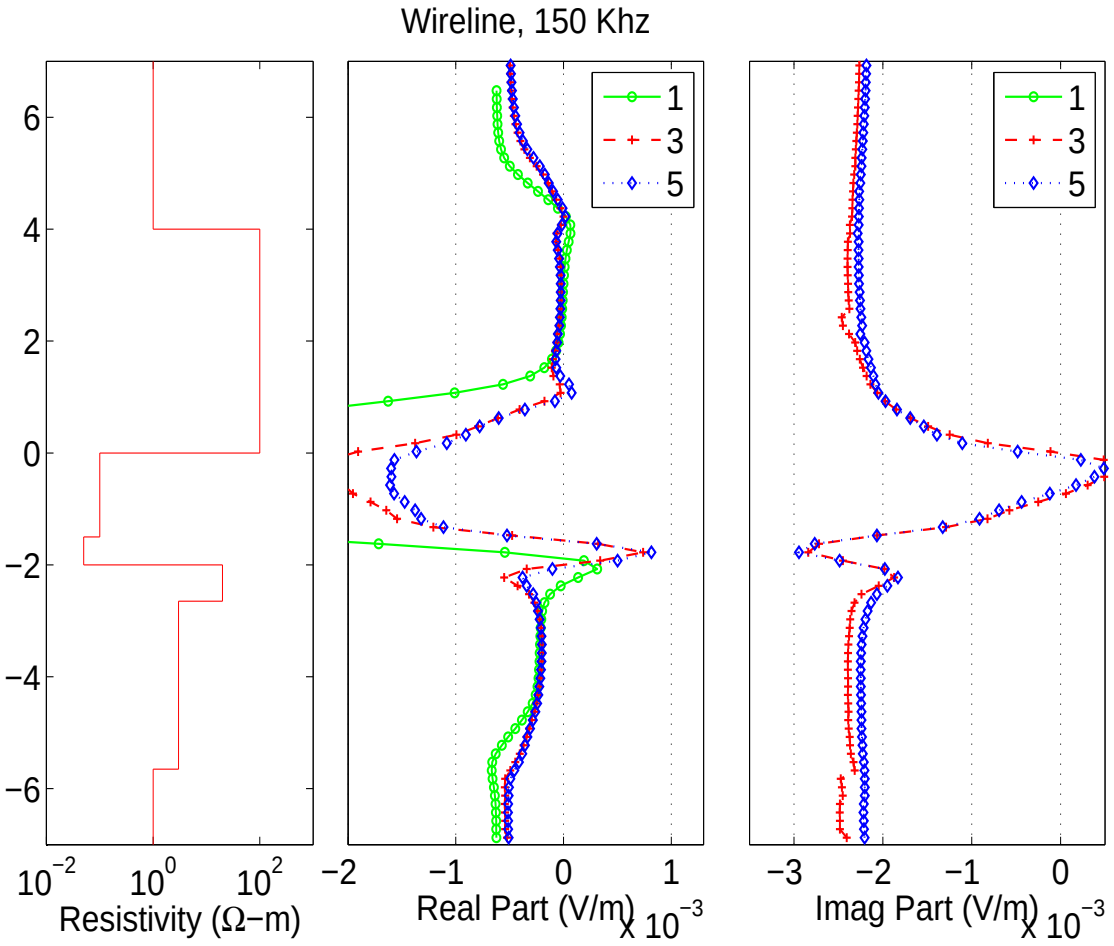

NUMERICAL RESULTS: AC RESULTS

Verification

Logging Instrument in a Homogeneous Formation

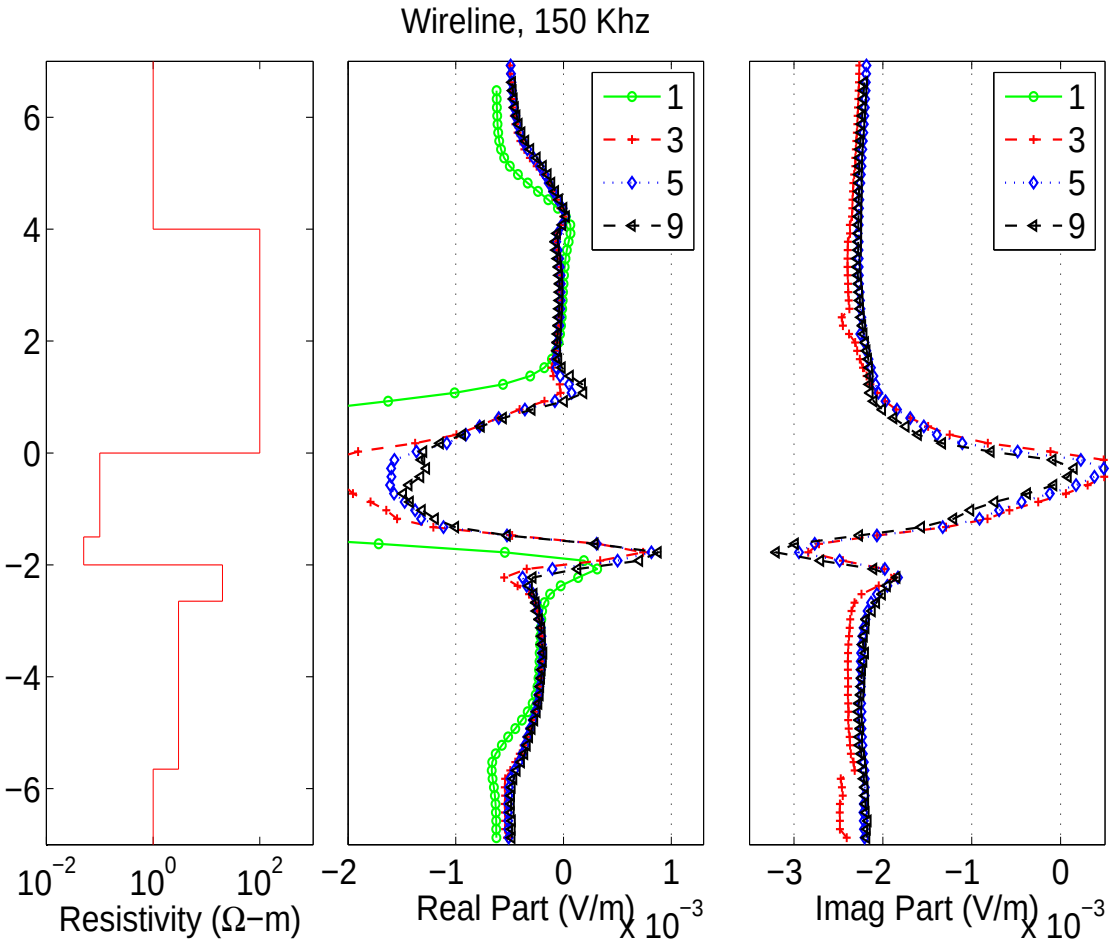

NUMERICAL RESULTS: AC RESULTS

Verification

Logging Instrument in a Homogeneous Formation

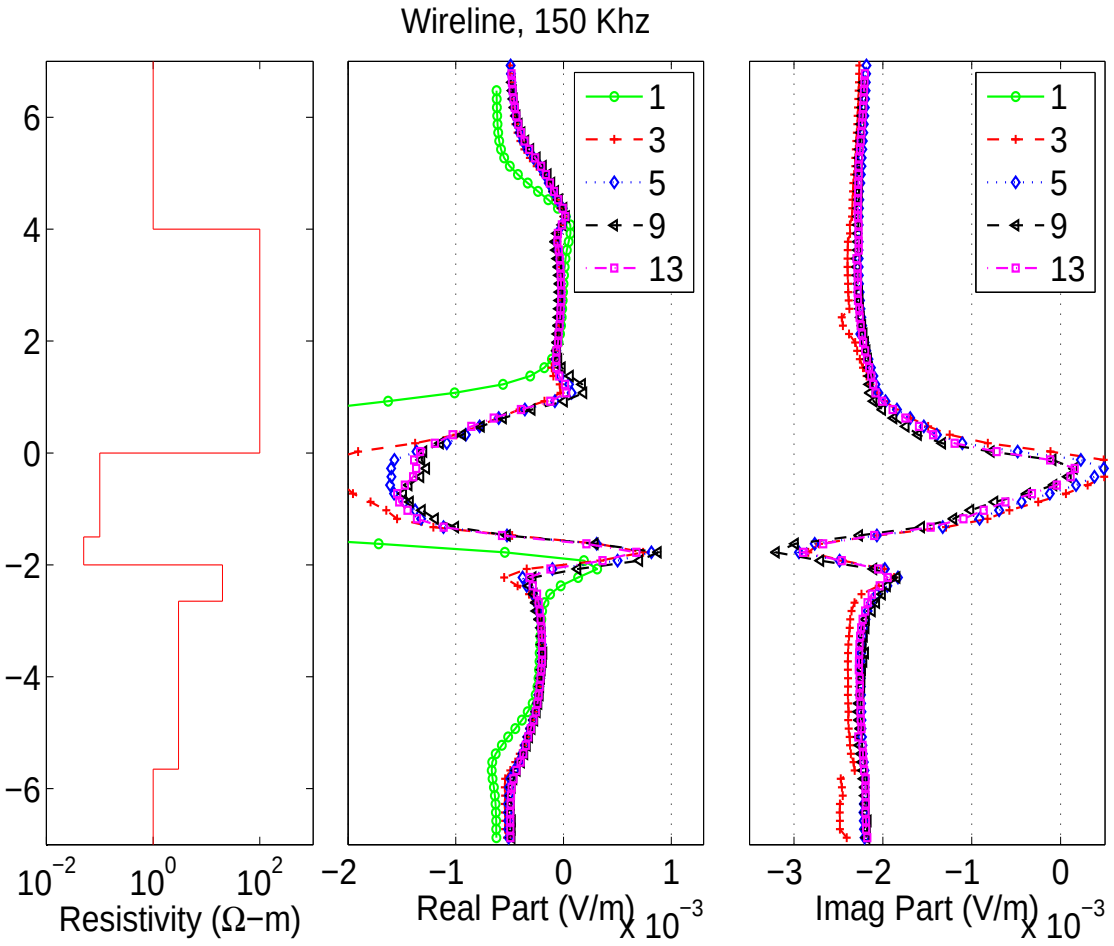

NUMERICAL RESULTS: AC RESULTS

Dip Angle

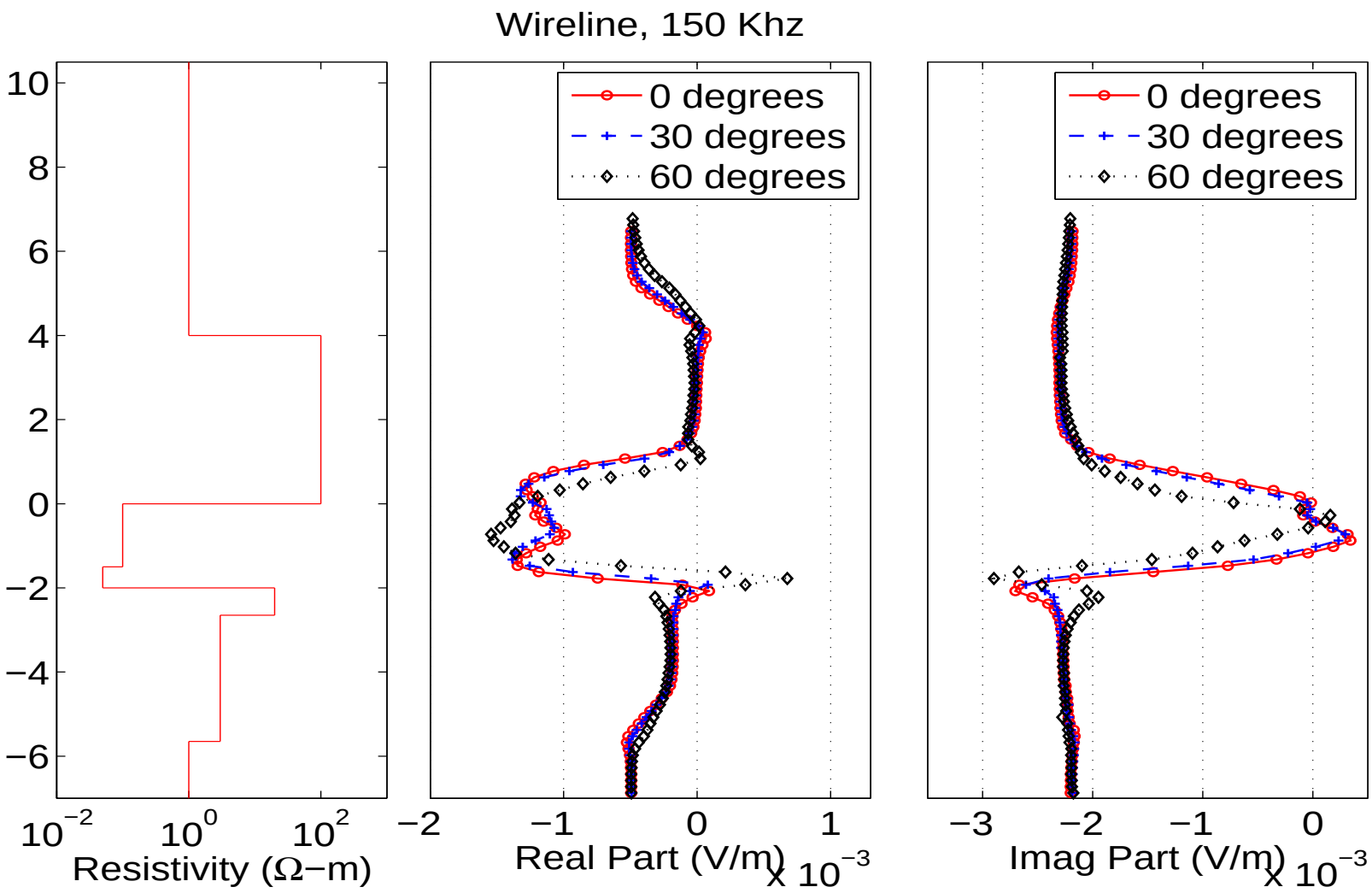

NUMERICAL RESULTS: AC RESULTS

Dip Angle + Invasion

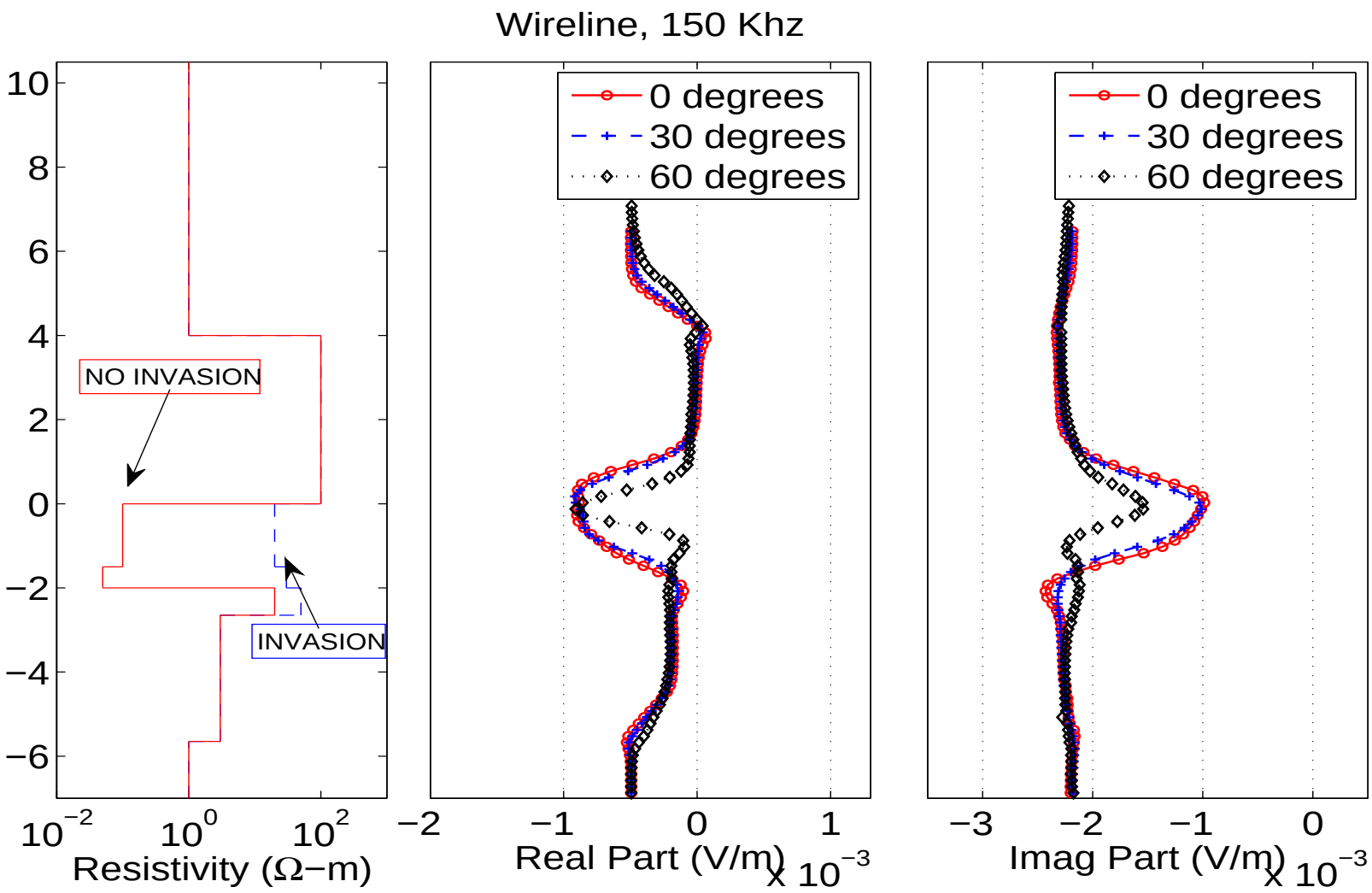

NUMERICAL RESULTS: AC RESULTS

Dip Angle + Anisotropy

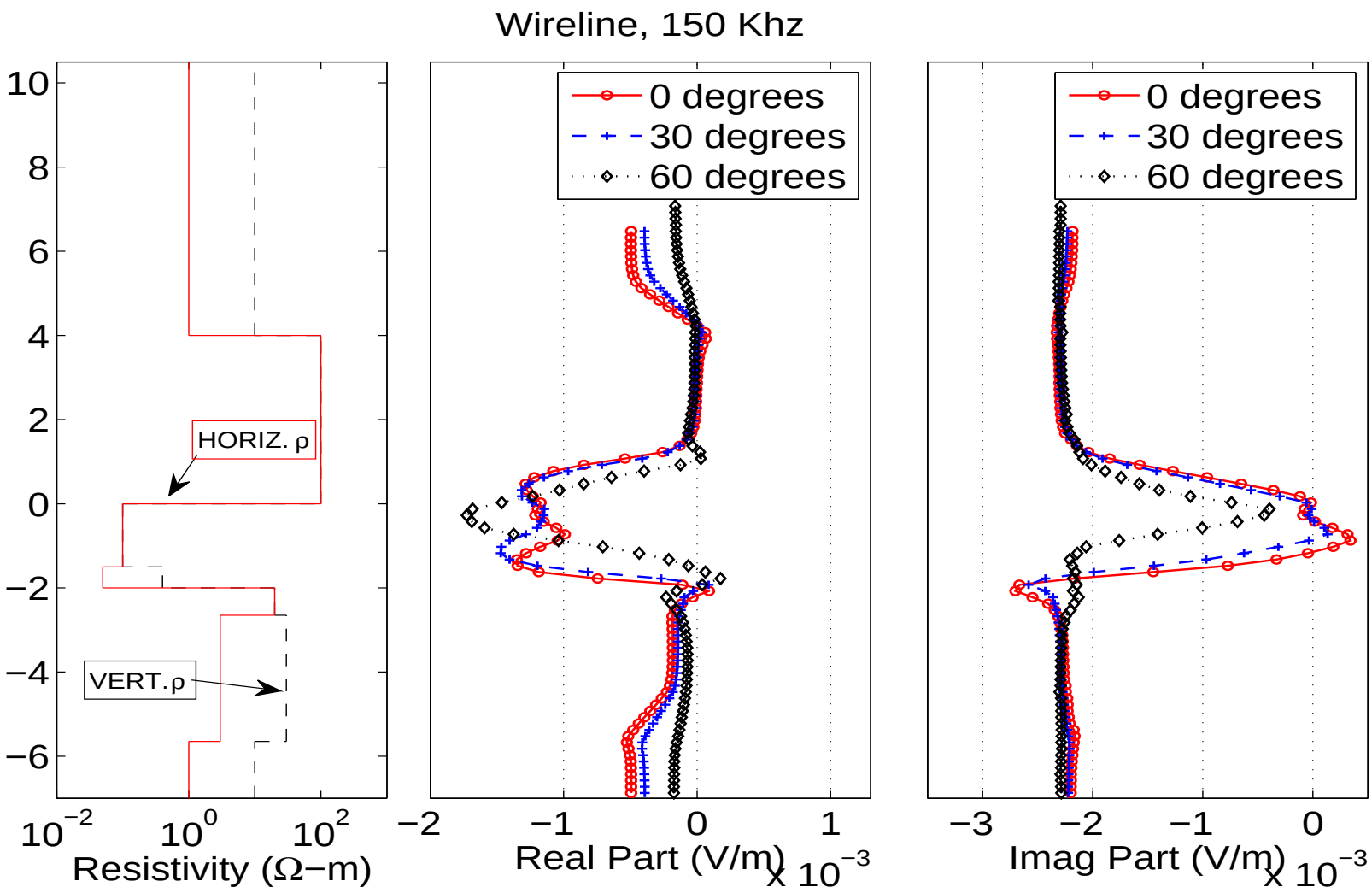

NUMERICAL RESULTS: AC RESULTS

Dip Angle + Invasion + Anisotropy

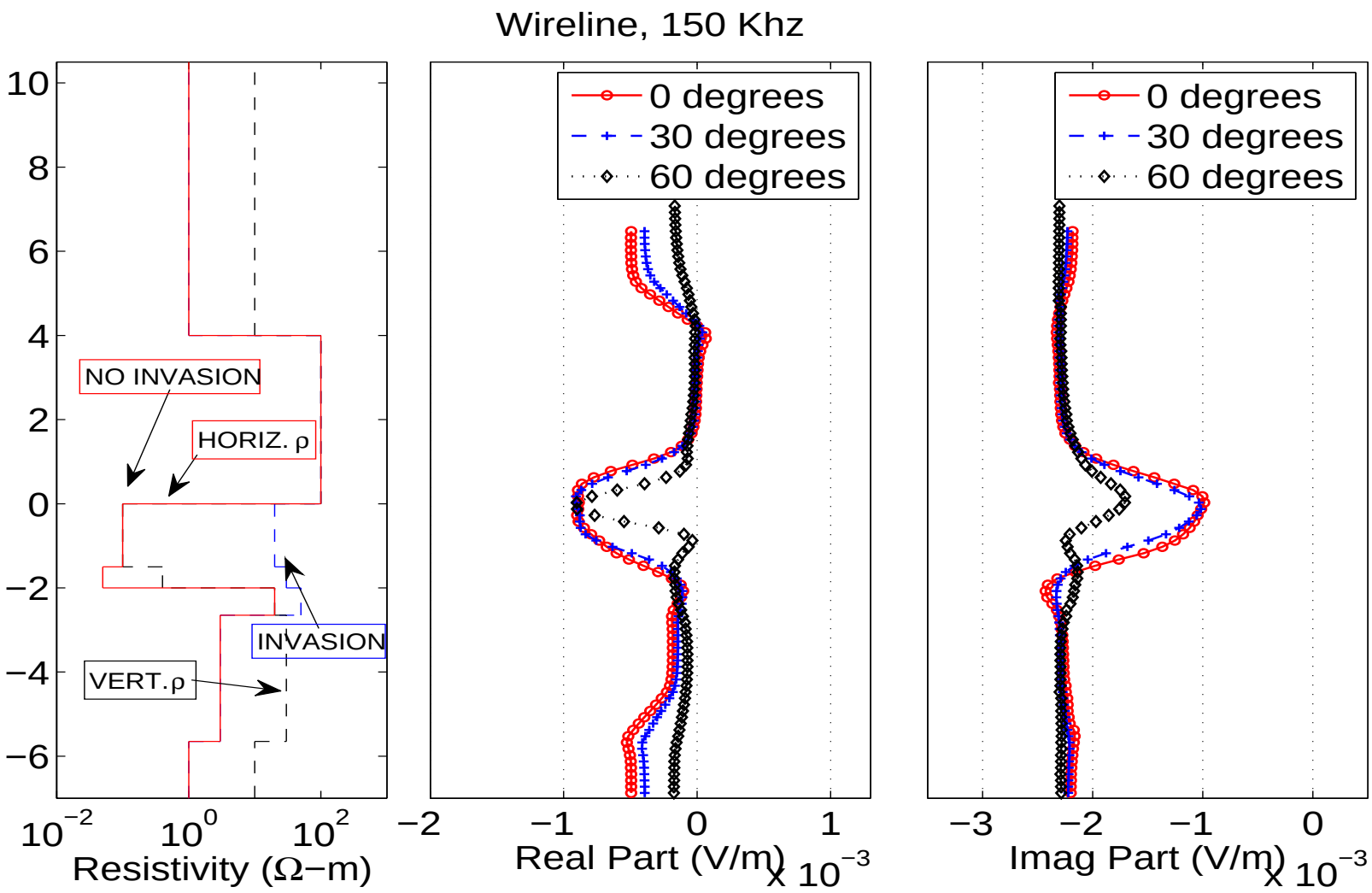

NUMERICAL RESULTS: AC RESULTS

60-Degree Deviated Well

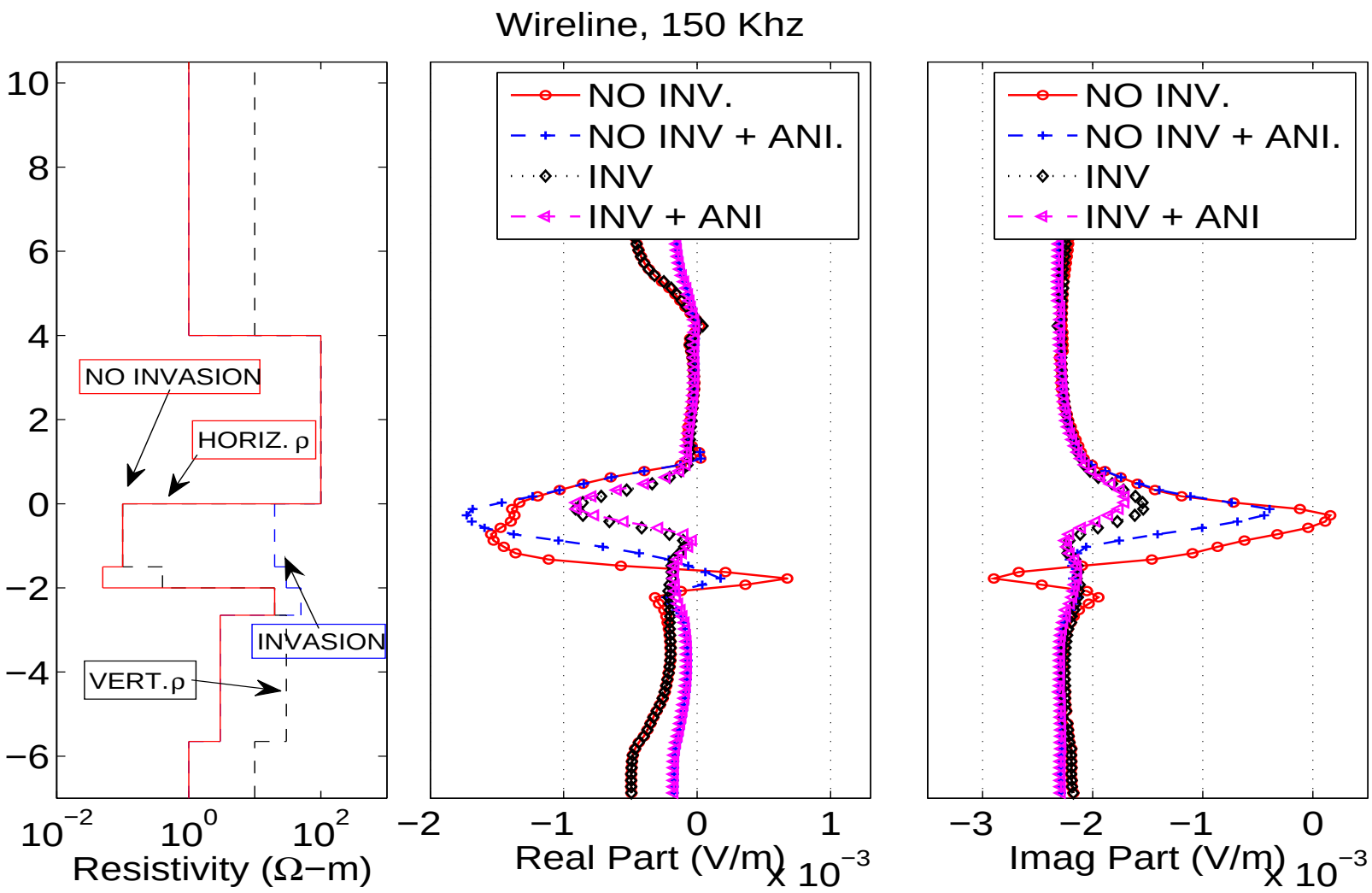

NUMERICAL RESULTS: AC RESULTS

Vertical Well with 0.03 m Eccentricity

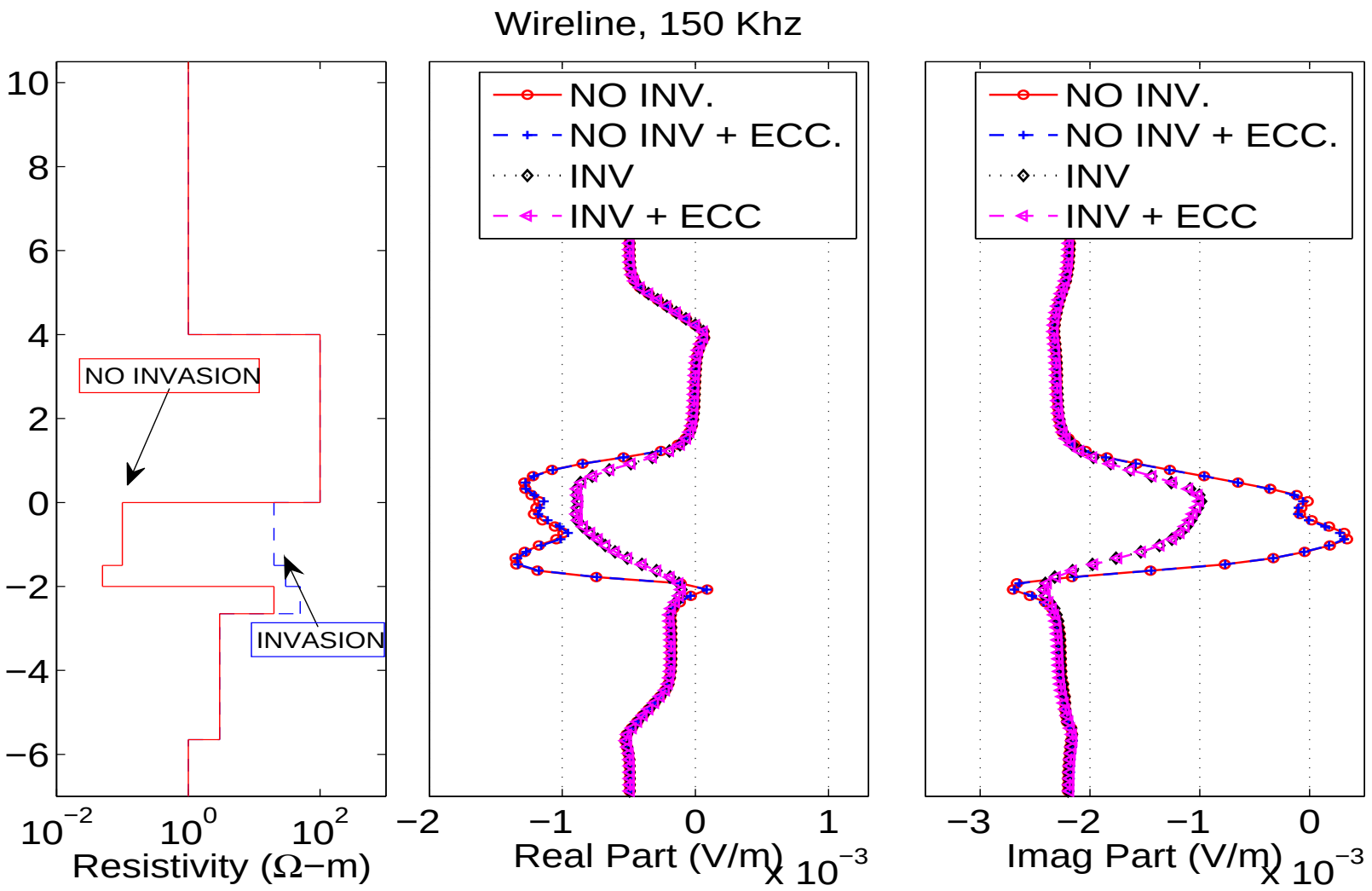

NUMERICAL RESULTS: AC RESULTS

Model Problem

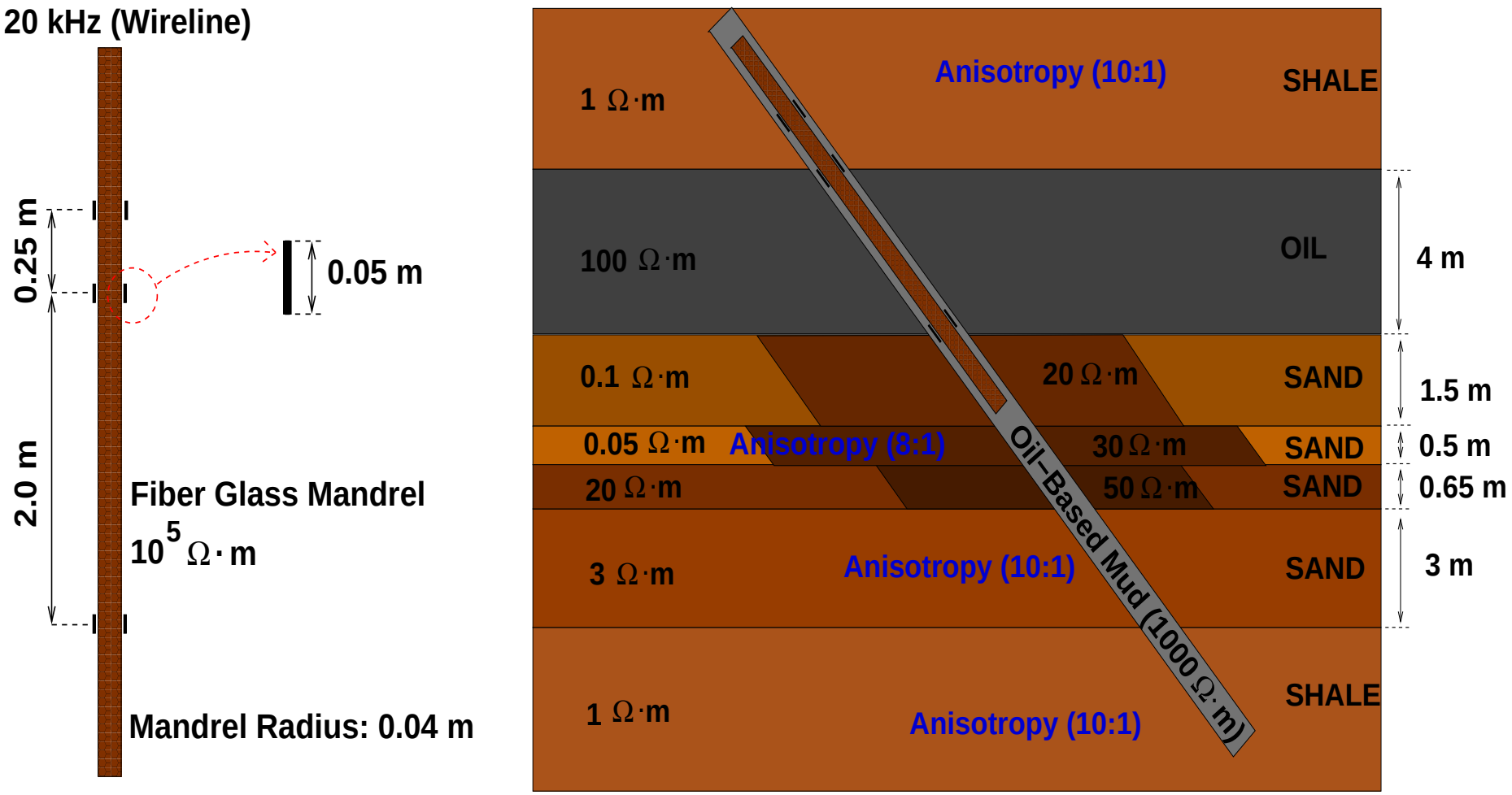

NUMERICAL RESULTS: AC RESULTS

Verification

Logging Instrument in a Homogeneous Formation

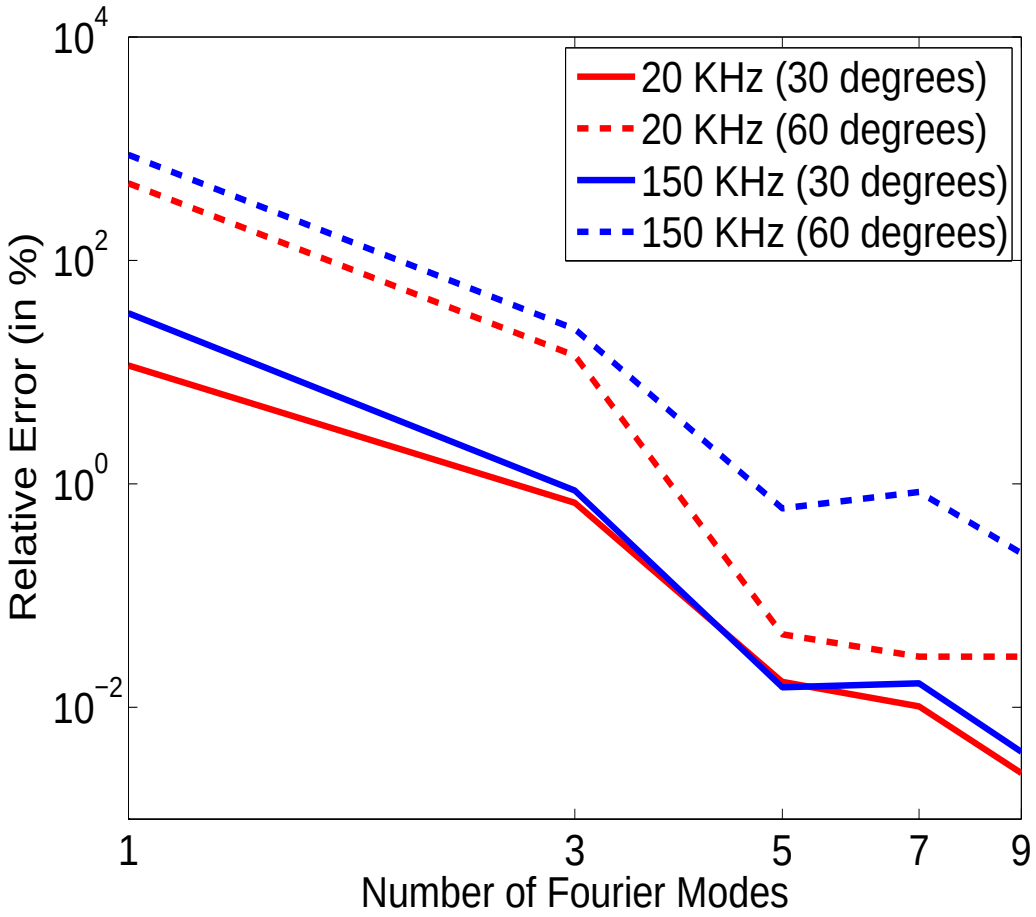

NUMERICAL RESULTS: AC RESULTS

Dip Angle

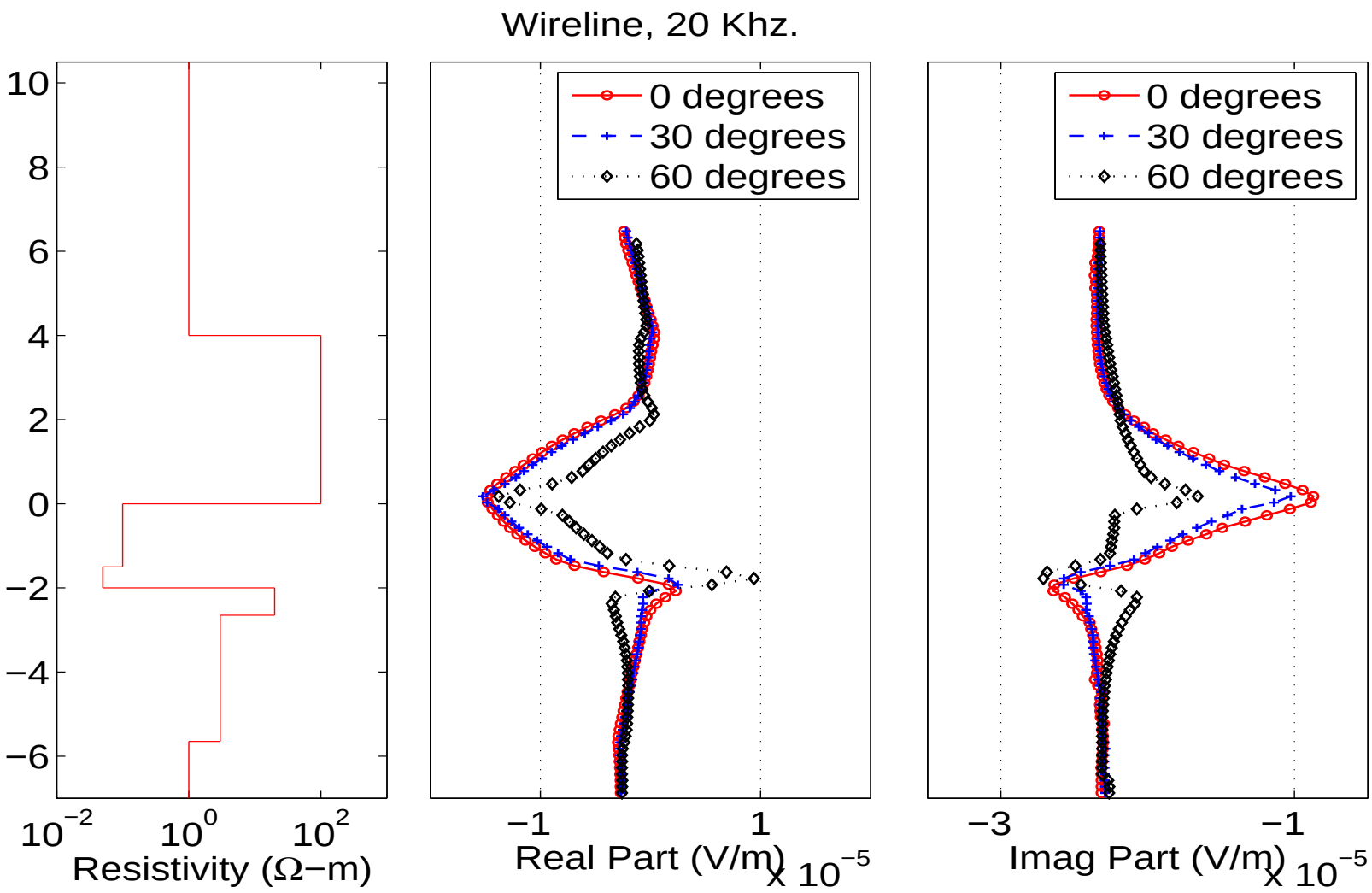

NUMERICAL RESULTS: AC RESULTS

Dip Angle + Invasion

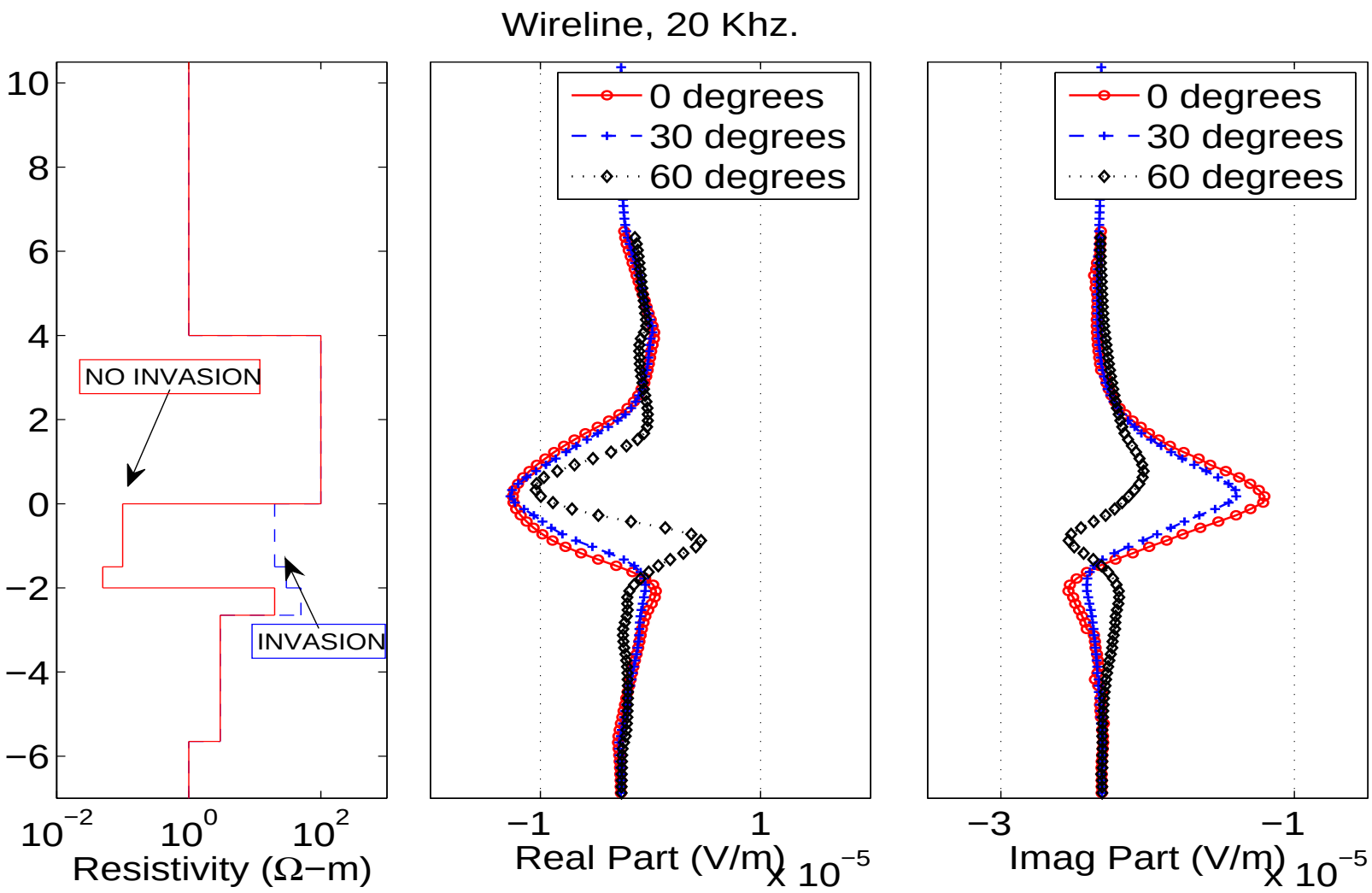

NUMERICAL RESULTS: AC RESULTS

Dip Angle + Anisotropy

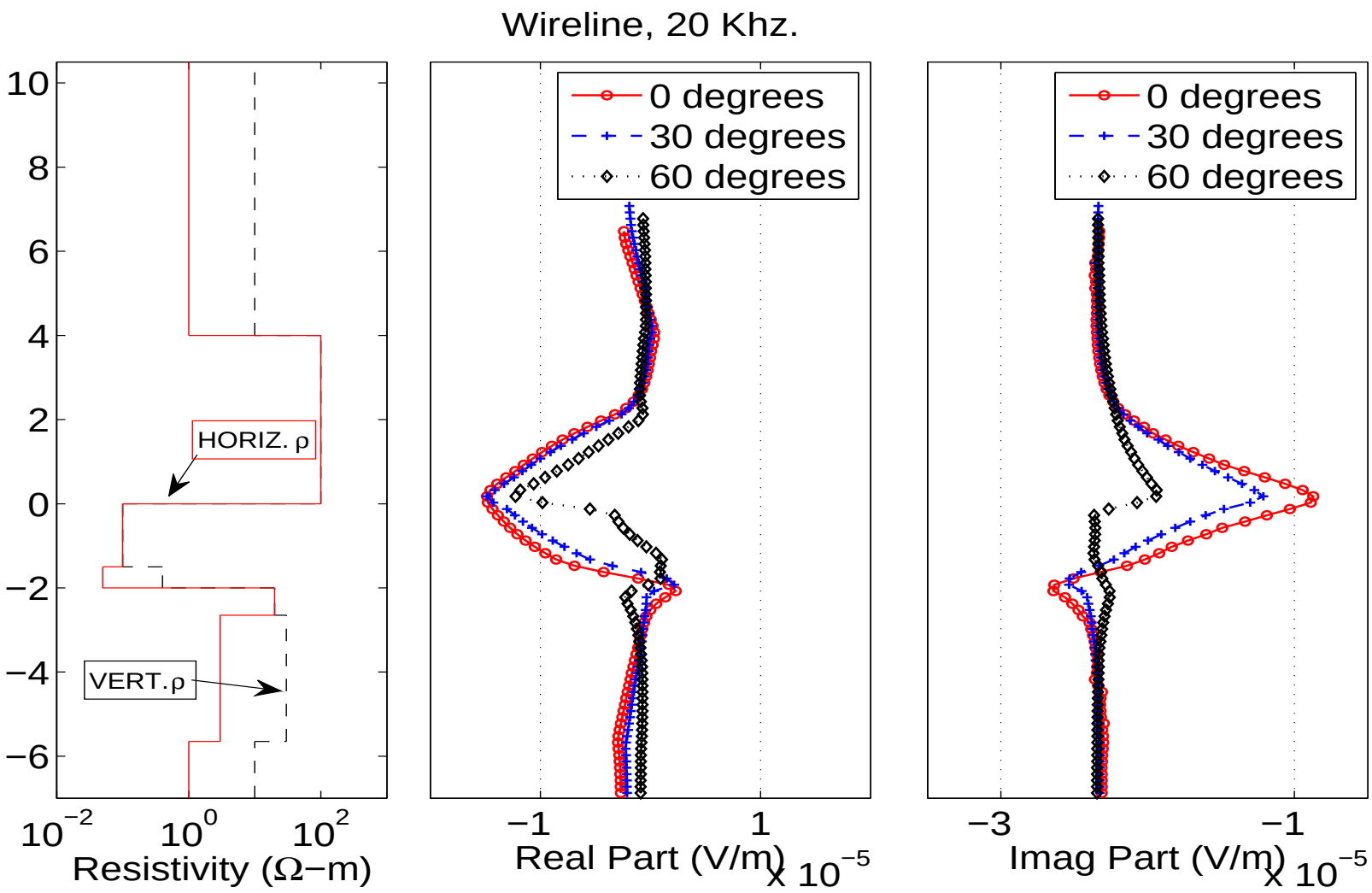

NUMERICAL RESULTS: AC RESULTS

Dip Angle + Invasion + Anisotropy

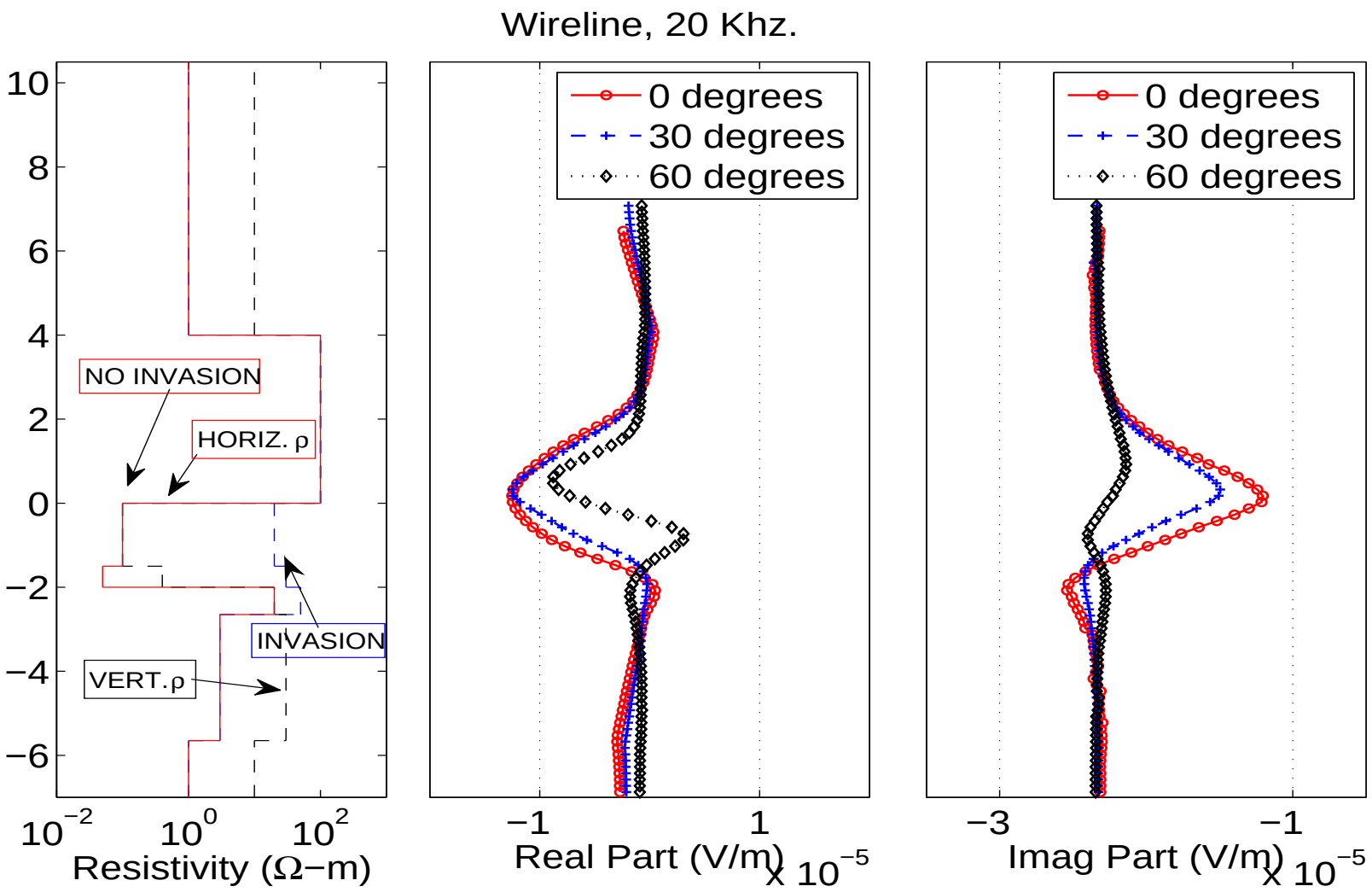

NUMERICAL RESULTS: AC RESULTS

60-Degree Deviated Well

Wireline, 20 Khz.

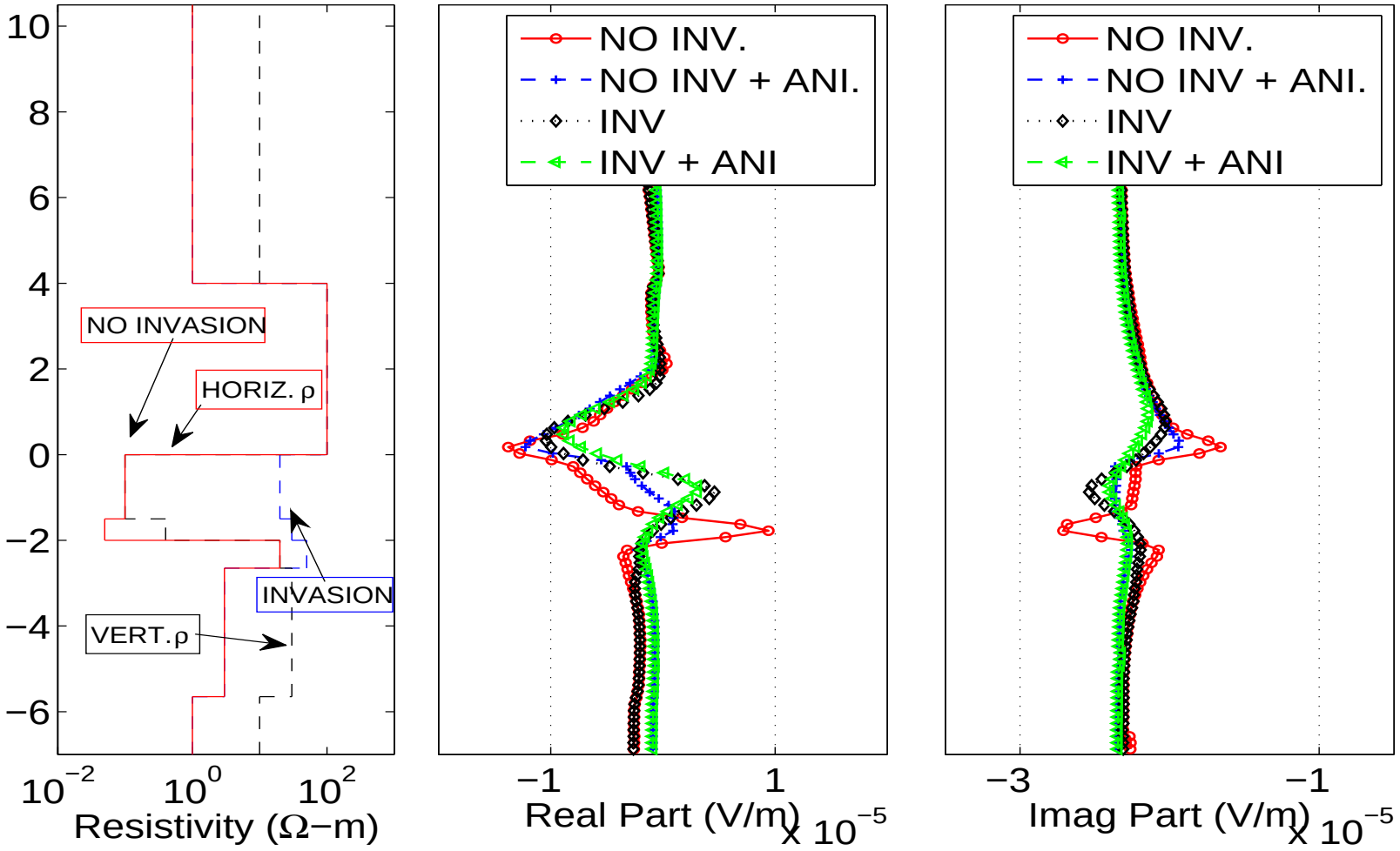

NUMERICAL RESULTS: LWD

Model Problem and Verification

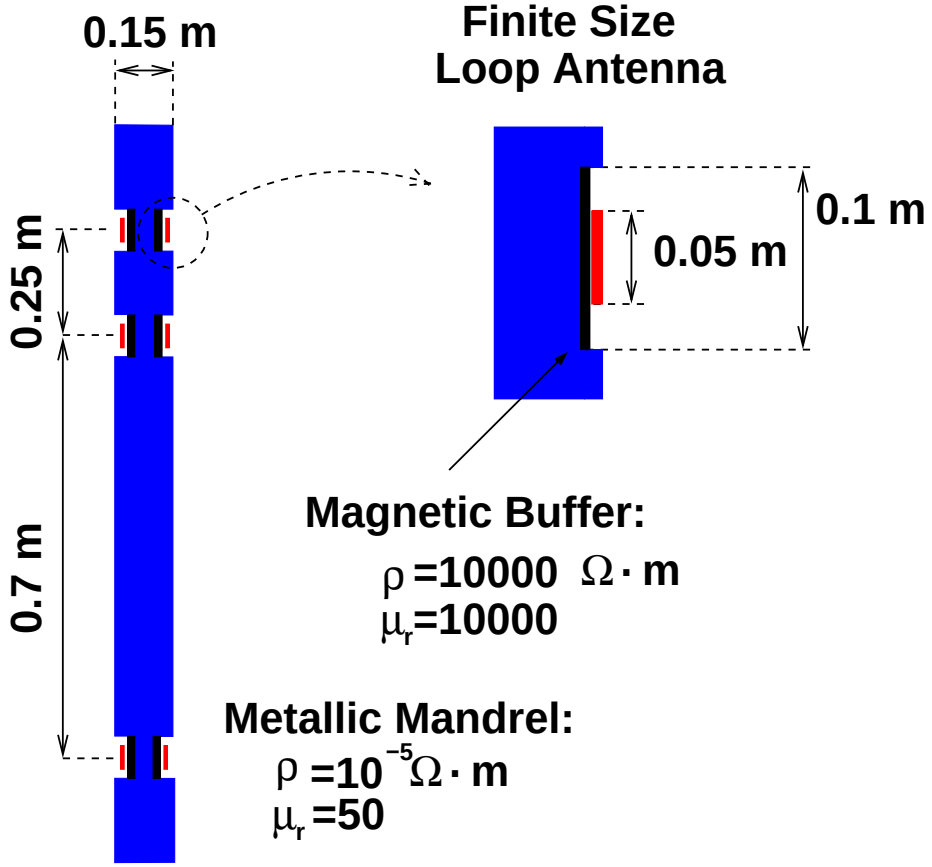

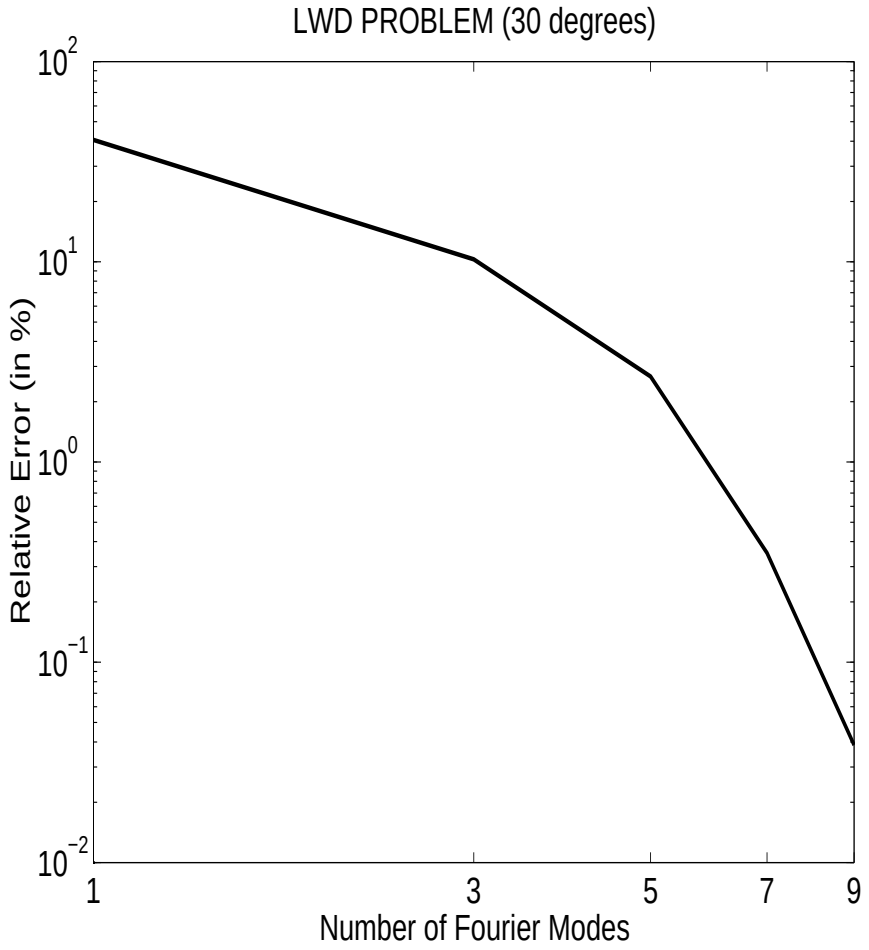

NUMERICAL RESULTS: LWD

Dip Angle

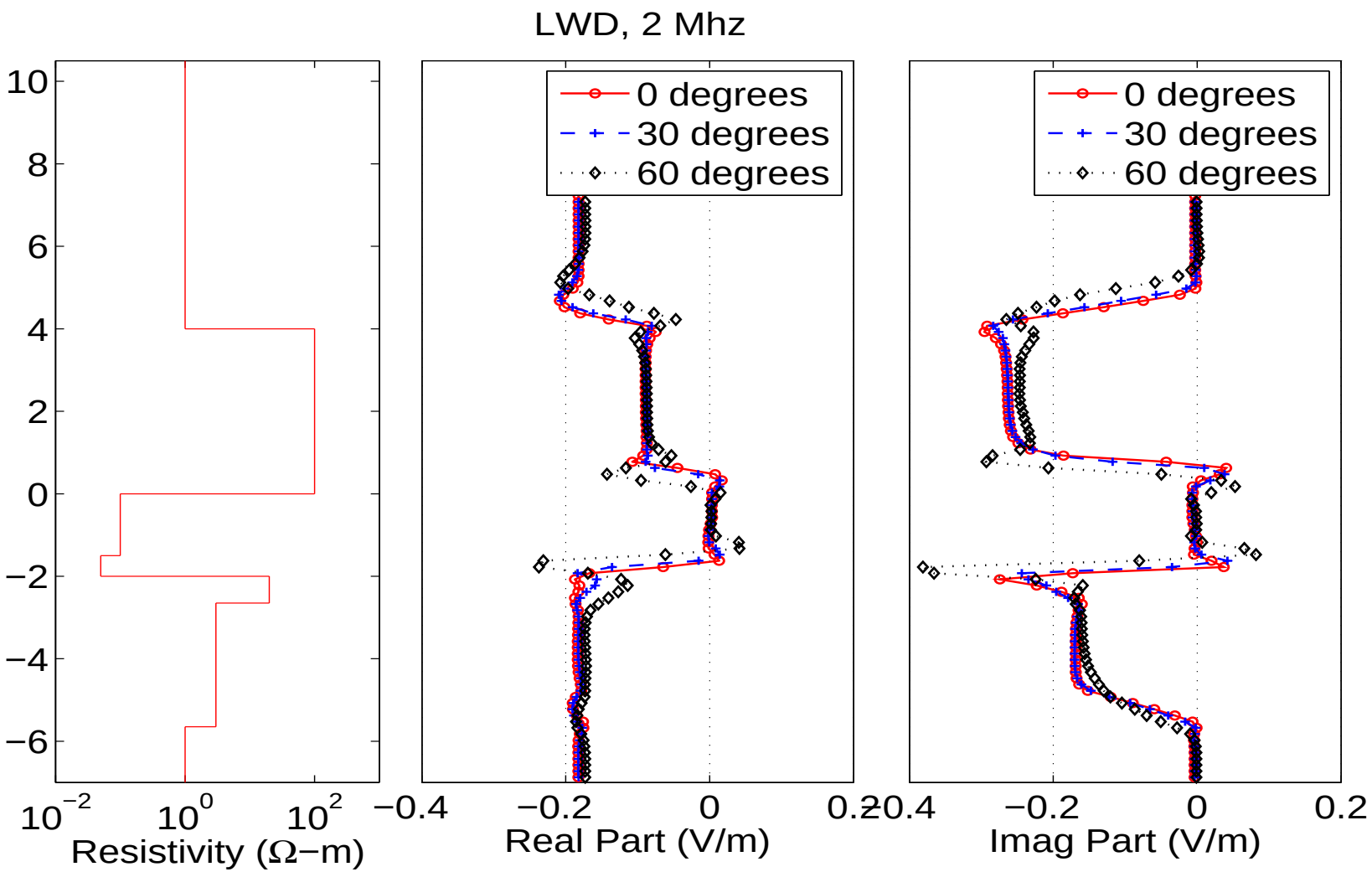

NUMERICAL RESULTS: LWD

Dip Angle + Invasion

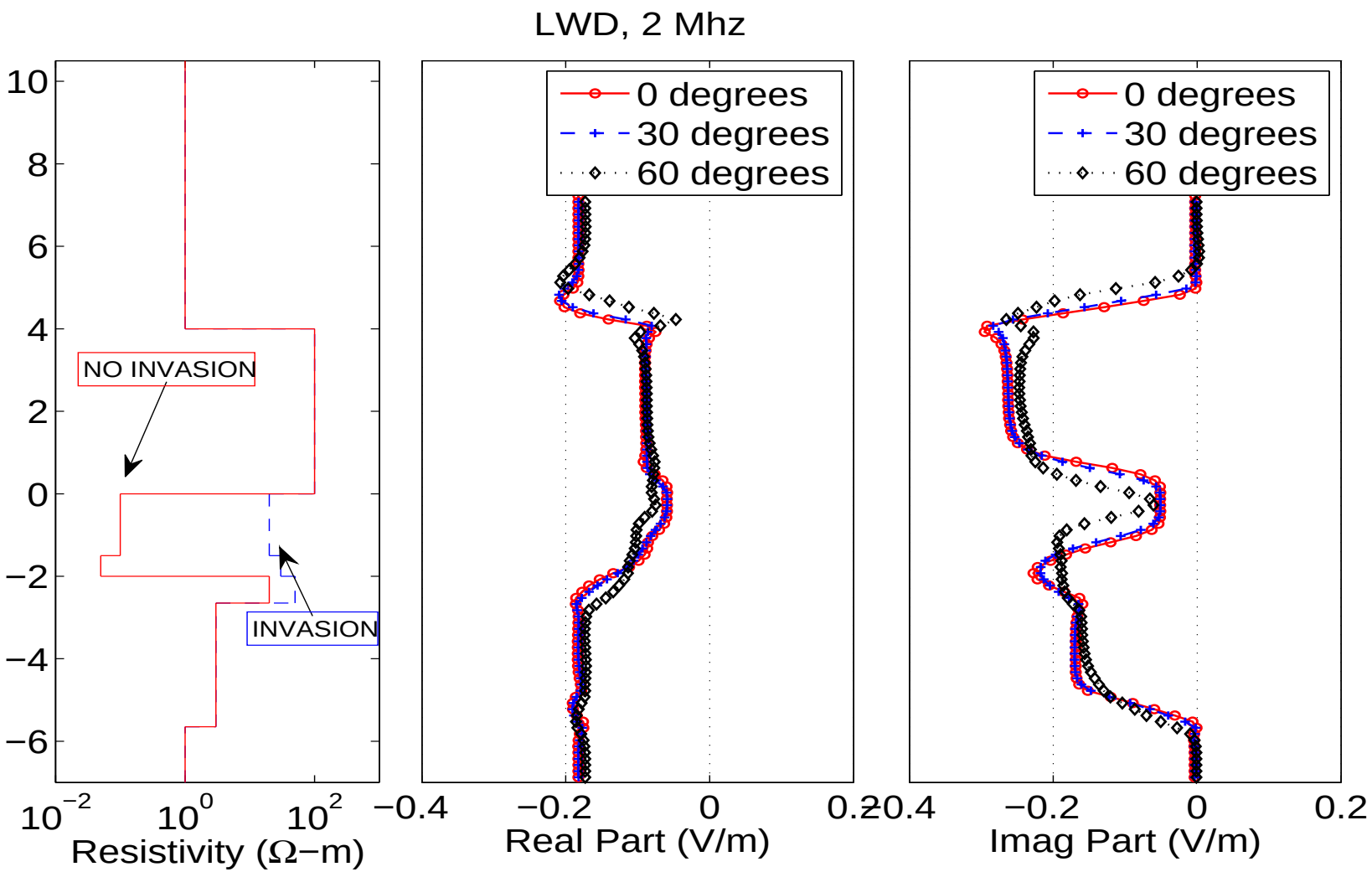

NUMERICAL RESULTS: LWD

Dip Angle + Anisotropy

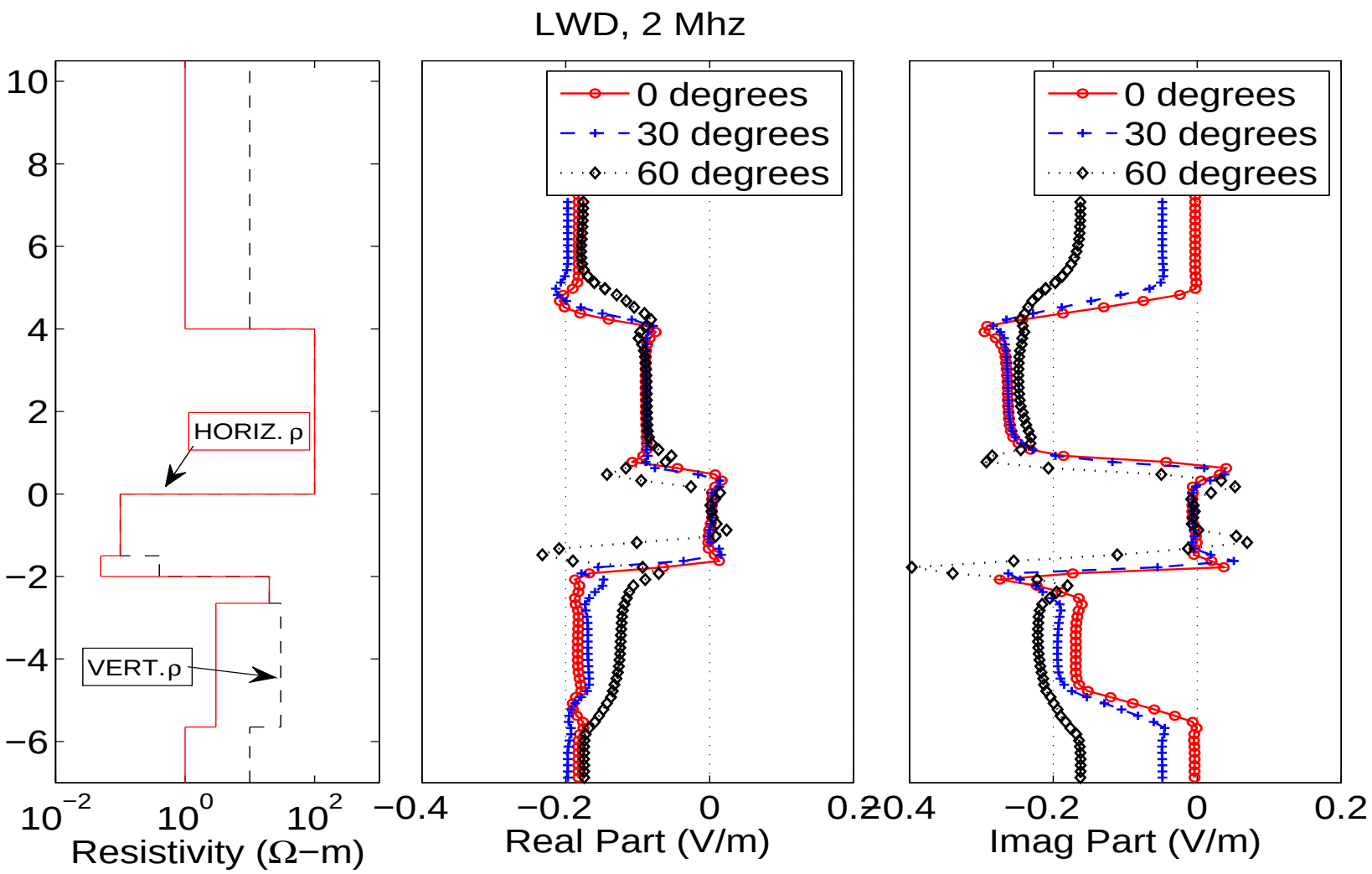

NUMERICAL RESULTS: LWD

Dip Angle + Invasion + Anisotropy

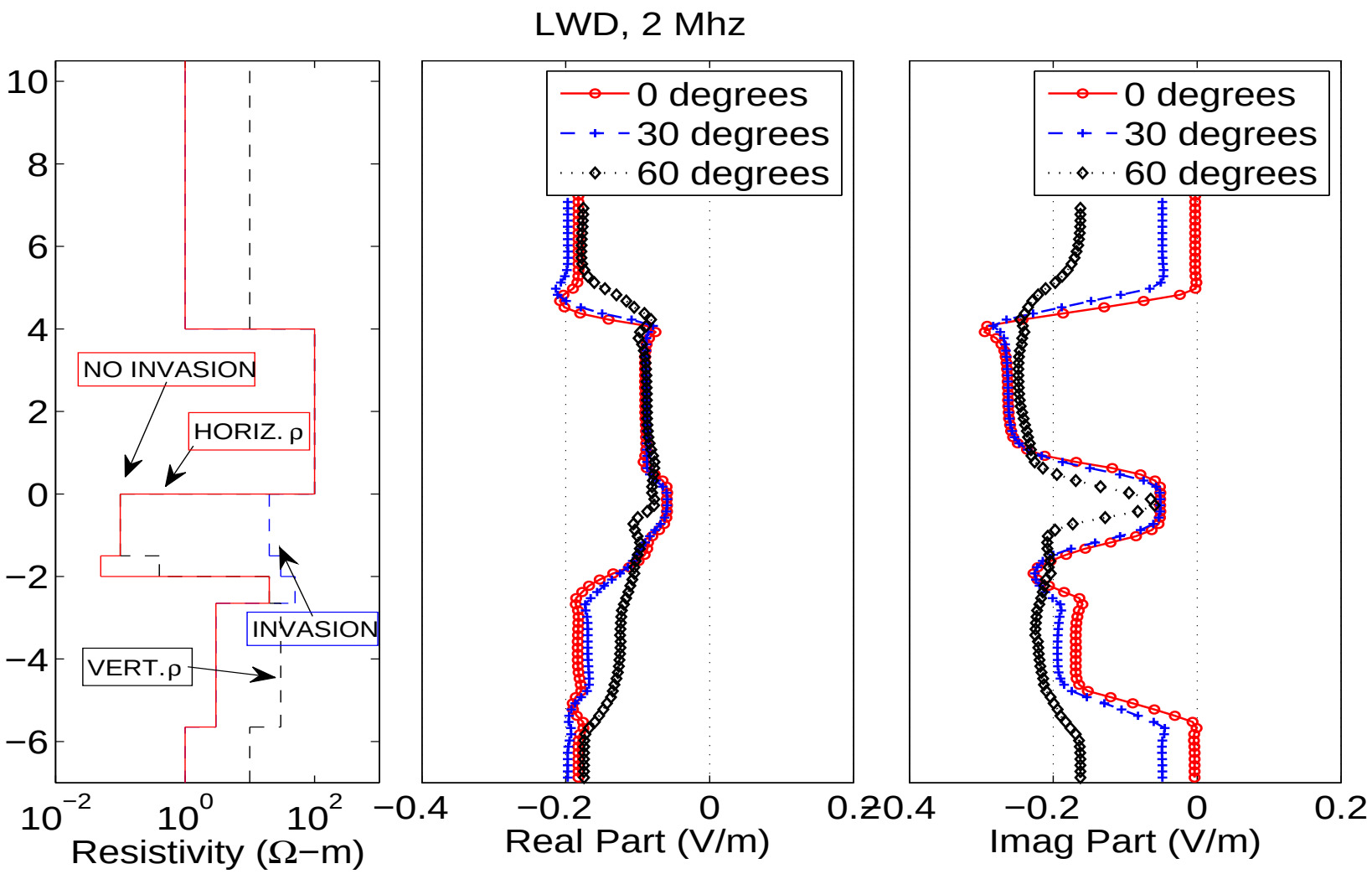

NUMERICAL RESULTS: LWD

60-Degree Deviated Well

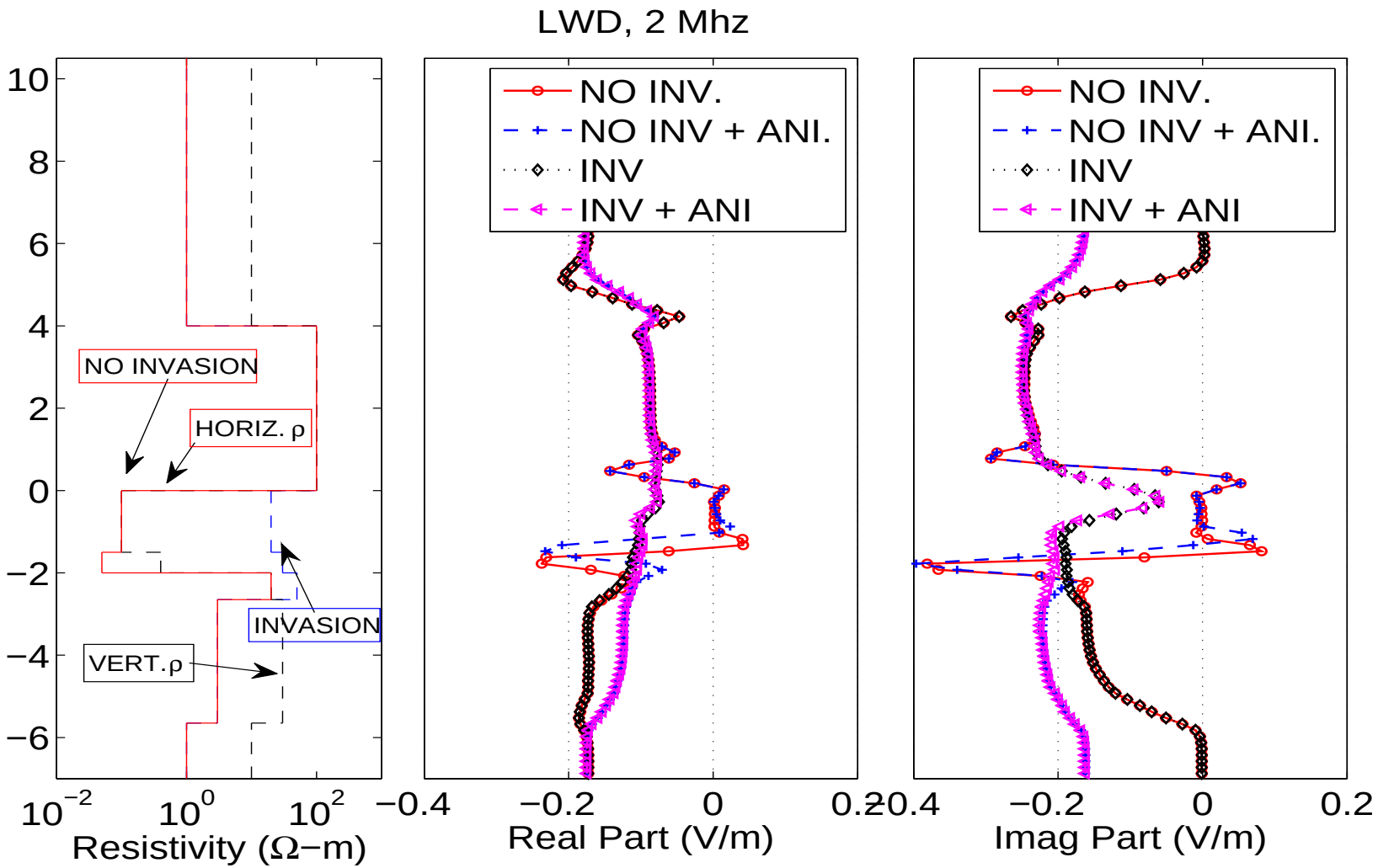

CONCLUSIONS AND FUTURE WORK

We have developed a new method based on a Fourier series expansion in a non-orthogonal system of coordinates.

- LIMITATION: Geometry of the problem.
- ADVANTAGE: It combines exponential convergence with sparse (penta-diagonal) matrices.
- FURTHER APPLICABILITY OF THE METHOD:
  - Eccentric measurements and tilted antennas.
  - Time-domain simulations.
  - Multi-Physics: Resistivity logging instruments, sonic logging instruments (acoustics + elasticity), fluid-flow, geomechanics, etc.
  - Inverse problems.
- FUTURE WORK: Iterative solver based on 2D-block Jacobi preconditioners.

ACKNOWLEDGMENTS

Sponsors of UT Consortium on Formation Evaluation